



**Warning and Mitigation Technologies for Travelling
Ionospheric Disturbances Effects**

TechTIDE

Report on the final TechTIDE products

Version 1.0

Grant agreement no: 776011

The TechTIDE has received funding from the European Commission Horizon 2020
research and innovation programme (2017 – 2020)



INDEX

Document Information.....	6
Abstract	6
Document history.....	6
Disclaimer	7
Executive Summary	7
1. Purpose and Scope of the Document	8
2. Associated documents.....	8
2.1. Applicable Documents	8
2.2. Reference Documents.....	8
2.3. Acronyms.....	9
3. TID detection methods: Final products and TID activity	10
3.1. HF-TID.....	13
3.2. HF-INT.....	14
3.3. Spatial and temporal GNSS analysis.....	16
3.4. GNSS TEC gradient	17
3.5. LS TID Index.....	18
3.6. HTI	20
3.7. CDSS-MSTID.....	22
3.8. AATR indicator.....	23
3.9. Ionospheric Background Conditions	24
3.10. Classification of the detection products and its categories for disturbance activity	25
4. Results of the TID methods and products in TechTIDE and TID impact on aerospace and ground systems	28
4.1. Impact of TechTIDE TID detection on aerospace systems.....	28
4.2. Impact of TechTIDE TID detection on ground systems.....	43
5. Summary and additional remarks.....	45



Index of Tables

Table 1.	List of applicable documents.....	8
Table 2.	List of reference documents	8
Table 3.	List of acronyms.....	9
Table 4.	Summary of TechTIDE TID identification methodologies. Green background: real-time capability, yellow: transition to real-time in progress.....	11
Table 5.	Information on the parameters/characteristics of the atmospheric wave activity as it is provided on the IAP CDSS website. Spectrogram on the left is visualization of the Doppler shift product as provided in the TechTIDE warning system for a given scenario.....	23
Table 6.	Levels of the disturbance activity for the Disturbance Indicators in TechTIDE. ..	25
Table 7.	Levels of the disturbance activity for the LSTID detection of TechTIDE.....	25
Table 8.	Levels of the disturbance activity for the MSTID detection of TechTIDE.....	26
Table 9.	Categories of the disturbance for the Disturbance Indicators	27
Table 10.	Categories of the disturbance for the LSTID Detection Methods.	27
Table 11.	Categories of the disturbance for the MSTID Detection Methods.....	28
Table 12.	List of scenarios analyzed comparing the EGNOS APV-I 99% Availability Degraded Area (EGNOS-D) with category of disturbances detected by the indicated TechTIDE methods/products.....	32
Table 13.	Percentage of Disturbed events detected by the respective TechTIDE method/products that coincide with degradation in the EGNOS performance (percentages in parenthesis refer to the ration of events when the particular method provide data) and with no with degradation in the EGNOS performance. Results in this table do not distinguish the degree of impact in the EGNOS performance. N/A means that no data is available for the given method/product.....	40
Table 14.	List of scenarios when HF-INT method detects the strongest LSTID events since 2018. Comparison with other TechTIDE detection methods and with the impact on EGNOS, based on APV-I 99% Availability Degraded Area (EGNOS-D) is provided. N/A means that no data was available for the given method/product.	41
Table 15.	Percent of scenarios reported in Table 14 with simultaneous TID detection by given methods. The last column reports the percent of scenarios that a given method detects TID activity and EGNOS performance is degraded.....	42
Table 16.	Analysis of the coincident TID events detected by HF-INT with DF measurements.....	44



Index of Figures

Figure 1. Example of the HF-TID product in the real-time TechTIDE warning service for a given scenario.....	14
Figure 2. Geographic locations of the Digisonde stations used in the HF-INT method for Europe (left) and South Africa (right) network.	15
Figure 3. Example of the HF-INT product in the real-time TechTIDE warning service for a given scenario over Europe network.	15
Figure 4. Distribution of the occurrence of events detected by the HF-INT method with HF-INT _{EUx} or lower.....	16
Figure 5. Example of the MSTID product in the real-time TechTIDE warning service for a given scenario.....	17
Figure 6. TEC gradients derived from IGS TEC maps in the European for a given scenario. The TEC gradients amplitude is given in mm/km.	18
Figure 7. The LSTID index over Dourbes for the interval 6-12 September 2017 presented together with the AATR index from high altitude stations and with indicative daily maps of EGNOS availability.	19
Figure 8. Examples of the electron density maps for given heights and given scenarios together with the corresponding RSTD (%) above given measuring sites (bottom-right).	20
Figure 9. Example of the HTI plots for various frequency bins shown as different colors. .	21
Figure 10. Statistical model fitting by combining all available frequency bins.	21
Figure 11. Daily HTI output over Juliusruh station for 12/12/2019.	22
Figure 12. Example of the AATR product in the real-time TechTIDE warning service for a given scenario.....	23
Figure 13. Maps of the residuals of the current electron density in respect to median conditions with color scales in respect to positive and negative effect. The Maps are calculated at 200km, 300km, 400km and 500 km. This example shows only the map at 200km (left) and 400km (right).	24
Figure 14. <i>APV-I availability at RIMS EGI (black), AATR values at IGS station ARG1 (purple) and REYK (green) from 7th to 9th September (DOY 250 – 252). Plot gathered from [RD-5].</i>	28
Figure 15. Example of a HF-TID event detection data for a given radio link (middle) compared with the EGNOS APV-I service degradation data (top).....	29



Figure 16. Example of a HF-INT event detection data for a given sensor located in Germany (middle) compared with the EGNOS APV-I service degradation data (top) and for a given scenario. 30

Figure 17. Comparison of the disturbance activity reported by the TechTIDE methods/products with EGNOS APV-I 99% Availability Degraded Area for 31st January 2017. 31

Figure 18. Histograms reporting the number of measurements (x-axis) observed with a given azimuth (y-axis). The different filters have been applied in the direction azimuth of the indicated HF Beacon and with the given aperture of sector as noted in the legend. 44

Figure 19. Distribution of the MSTID events detected by the MSTID_x (left) and of the LSTID events detected by HF-INT_{EUx} (right) for 2017. 45



Document Information

Deliverable number:	D2.3
Deliverable title:	Report on final TechTIDE products
Date of Delivery:	31 st December 2019
Author(s):	OE, BGD, NOA, DLR, FU, UPC, IAP
Work Package no.:	2
Work Package title:	TID Activity Report
Work Package leader:	OE
Dissemination level:	Public
Nature:	Report

Abstract

The deliverable presents a report on the final products in TechTIDE. The TID identification codes in TechTIDE have been adjusted since its first release driven by the assessment of the TID impact on aerospace and ground systems (WP5) to efficient support specific systems operations (such EGNOS, N-RTK, HF communication and geolocation) and the mitigation of the TID effects. The new products and improvements resulted of users' recommendations and WP5 results. The final TechTIDE products released after this adjustment, are described in this report.

Document history

Version	Date	Edited by	Reason for modification / Remarks
0.0	13.12.2019	D. Altadill, E.Blanch, A. Segarra, J. Chum, Ch. Timoté, I. Galkin, A. Belehaki, C. Borries.	Initial Draft / To WP2 for review
1.0	20.12.2019	D. Altadill, E.Blanch, A. Segarra, J. Chum, Ch. Timoté, I. Galkin, A. Belehaki, C. Borries, H. Haralambous.	To EB for review



Disclaimer

This document contains description of the TechTIDE project findings, work and products. Certain parts of it might be under partner Intellectual Property Right (IPR) rules so, prior to using its content please contact the Project Coordinator (Dr Anna Belehaki, belehaki@noa.gr) for approval.

In case you believe that this document harms in any way IPR held by you as a person or as a representative of an entity, please do notify us immediately.

The authors of this document have taken all reasonable measures in order for its content to be accurate, consistent and lawful. However, neither the project consortium as a whole nor the individual partners that implicitly or explicitly participated in the creation and publication of this document hold any sort of responsibility that might occur as a result of using its content.

This publication has been produced with the assistance of the European Union. The content of this publication is the sole responsibility of the TechTIDE consortium and can in no way be taken to reflect the views of the European Union.

Executive Summary

TechTIDE project, funded by the European Commission Horizon 2020 research and innovation program [AD-1], will establish a pre-operational system to demonstrate reliability of a set of TID (Travelling Ionospheric Disturbances) detection methodologies to issue warnings of the occurrence of TIDs over the region extended from Europe to South Africa. TechTIDE warning system will estimate the parameters that specify the TID characteristics and the inferred perturbation, with all additional geophysical information to the users to help them assess the risks and to develop mitigation techniques, tailored to their application. This document is a report for the final products and improvements provided by TID identification codes in TechTIDE after its adjustment since its first release which resulted of users' recommendations and WP5 results.

1. Purpose and Scope of the Document

This document presents the final products of the TID identification codes in TechTIDE released after adjustments driven by WP5 (Assessment of the TID impact on aerospace and ground systems) results, to efficient support specific systems operations (such EGNOS, N-RTK, HF communication and geolocation) and the mitigation of the TID effects. The document is divided into four sections:

Section 1 (the current section) describes the purpose of this document and its organization.

Section 2 lists the applicable and reference documents and also contains the list of acronyms used in this document.

Section 3 presents a summary of the TIDs methods and products in TechTIDE, the classification and the categories of the TID activity for the respective methods, with especial emphasis on new developments and improvements since the first release of TechTIDE warning system.

Section 4 presents results of the TID methods and products in TechTIDE to support specific systems operations as concerns the TID impact on aerospace and ground systems.

Section 5 is the summary and includes some additional remarks.

2. Associated documents

2.1. Applicable Documents

The following table contains the list of applicable documents.

Table 1. List of applicable documents

AD	Document title
[AD-1]	Grant Agreement number: 776011 — TechTIDE — H2020-COMPET-2017

2.2. Reference Documents

The following table contains the list of references used in this document.

Table 2. List of reference documents

RD	Document title
[RD-1]	Warning and Mitigation Technologies for Travelling Ionospheric Disturbances Effects TechTIDE D2.1 Report on the design and specifications of the TID algorithms and products
[RD-2]	Warning and Mitigation Technologies for Travelling Ionospheric Disturbances Effects TechTIDE D2.2 Report on TID algorithms
[RD-3]	Warning and Mitigation Technologies for Travelling Ionospheric Disturbances Effects TechTIDE D3.2 Report on TID drivers

RD	Document title
[RD-4]	Warning and Mitigation Technologies for Travelling Ionospheric Disturbances Effects TechTIDE D3.5 Report on TID activity metrics definition
[RD-5]	Warning and Mitigation Technologies for Travelling Ionospheric Disturbances Effects TechTIDE D5.2 Statistical Analysis of the Results
[RD-6]	Kutiev, I., P. Marinov, and A. Belehaki (2016), Real time 3-D electron density reconstruction over Europe by using TaD profiler, Radio Sci., 51, doi:10.1002/2015RS005932.
[RD-7]	Juan J.M, J. Sanz. A. Rovira-García, G. González-Casado, D. Ibáñez and R. Orús Pérez (2018). AATR an ionospheric activity indicator specifically based on GNSS measurements. J. Space Weather Space Clim. 2018, 8, A14. doi.org/10.1051/swsc/2017044 .
[RD-8]	Hooke, W. H., Ionospheric irregularities produced by internal atmospheric gravity waves, J. Atmos. Sol. Terr. Phys., 30, 795– 823, 1968.
[RD-9]	Warning and Mitigation Technologies for Travelling Ionospheric Disturbances Effects TechTIDE D4.3 TechTIDE warning system. Second Release

2.3. Acronyms

The following table contains the list of all acronyms used in this document.

Table 3. List of acronyms

Acronym	Definition
2D	2-Dimension
3D	3-Dimension
AATR	Along-arc TEC rate
BGD	Borealis Global Designs Ltd.
CDSS	Continuous Doppler Sounding System
DLR	German Aerospace Center
DPS4D	Digisonde-Portable-Sounder-4D
EDD	electron density distribution
EGNOS	European Geostationary Navigation Overlay Service
FU	Frederick University
GBAS	Ground Based Augmentation System
GNSS	Global Navigation Satellite System

Acronym	Definition
HF	High Frequency
HF-INT	HF-Interferometry
HTI	Height-time-reflection intensity
IAP	Institute of Atmospheric Physics (Academy of Sciences of Czech Republic)
IdN	Identification Number
LSTID	Large Scale TID
MSTID	Medium Scale TID
MUF	Maximum Usable Frequency
NOA	National Observatory of Athens
OE	Fundació Observatori de l'Ebre
OI	Oblique Incidence
OTHR	Over The Horizon Radar
PFA	Probability of false alarm
POD	Probability of detection
ROT	Rate of TEC
Rx	Receiver
SNR	Signal-to-Noise Ratio
SSA SWE	Space Situational Awareness Space Weather
SSBC	Solar Sector Boundary Crossing
SSN	Sunspot Number
TEC	Total Electron Content
TID	Travelling Ionospheric Disturbance
Tx	Transmitter
UPC	Universitat Politècnica de Catalunya
VI	Vertical Incidence
WP	Work-package

3. TID detection methods: Final products and TID activity

This section presents the TIDs algorithms in TechTIDE, as summarized in Table 4. Detailed description of the original concept, design, and first updates for each of the methodologies is provided in TechTIDE Deliverable D2.1 [RD-1] and Deliverable D2.2 [RD-2].

Table 4. Summary of TechTIDE TID identification methodologies. Green background: real-time capability, yellow: transition to real-time in progress.

IdN. Method	Main Characteristics	Intermediate Product	Final Product	Value added Product
1. HF-TID Detects perturbations in space from all possible sources (solar and lower atmosphere origin) and it is suitable for the identification of both MS and LS TIDs	<u>Input:</u> signal properties from Digisonde synchronized operation. <u>Output:</u> TID velocity, amplitude, propagation direction at the signal reflection point between the stations	Doppler frequency, angle of arrival, and time-of-flight from Tx to Rx, both OI and VI sounding	Separately for MS and LS TID: 1+ detections of {TID Period, Phase Velocity, Direction of propagation, Wavelength, and Amplitude}	Maps of the current TID activity Maps of TID occurrence probability
2. HF-INT Finds oscillation activity in ionospheric characteristics and it can detect LSTIDs only.	<u>Input:</u> ionospheric characteristics from VI and OI soundings. <u>Output:</u> 2D TID vector velocity, amplitude and period.	De-trended ionospheric characteristics and contribution of LSTID to the data variability.	Dominant period, Amplitude and 2D Vector velocity of detected LSTID.	Estimation of propagation of LSTIDs
3. MSTID index Can detect perturbations in space from all possible sources (solar and lower atmosphere origin) and it is suitable for the identification of MSTIDs	<u>Input:</u> GNSS TEC from single receivers over a region. <u>Output:</u> Fluctuations associated to the MSTIDs and estimation of the propagation parameters (direction, velocity and amplitude).	De-trended GNSS data measurements.	TID Velocity, Direction of propagation and Amplitude	Climatology and physical origin of MSTID
4. GNSS TEC Gradient Analyze TEC maps and it is mostly sensitive to perturbations from LSTIDs.	<u>Input:</u> Grids of TEC maps over a region. <u>Output:</u> Latitude-time maps of TEC gradients and indication of significant gradients.	Maps of TEC and TEC rate	TEC Gradients	Graphical presentation in an image
5. Single location LSTID index The index is derived comparing the detrended electron density with the standard deviation of the values included in the median calculation.	<u>Input:</u> the electron density distribution calculated with the TaD code over each Digisonde. <u>Output:</u> The detrended electron density (dNe) at various altitudes.	The relative standard deviation of the dNe values, RSDNe.	The relative standard deviation, RSDNe, at pre-defined heights (200, 300, 400, 500 km).	LSTID activity index at pre-defined heights (200, 300, 400, 500 km).

IdN. Method	Main Characteristics	Intermediate Product	Final Product	Value added Product
6. HTI Detects LSTID activity in the F-layer virtual height over a Digisonde station.	<u>Input:</u> raw vertical ionogram binary data from a single Digisonde station <u>Output:</u> Period and virtual height amplitude of LSTID activity over the Digisonde station.	F region virtual height variation above a Digisonde station	Period and virtual height amplitude of dominant LSTID activity.	Map indicating LSTID periodicity over various Digisonde stations
7. CDSS-MSTID Analyze Doppler shift of radio signals to detect quasi-periodic perturbations and associate them with overpassing MSTIDs.	<u>Input:</u> CDSS reflected signals, ionospheric characteristics and irregularities. <u>Output:</u> Doppler shift, SNR and confidence level.	Continuous Doppler shifts of fixed sounding radio frequency.	Period, Amplitude and Phase of Doppler measurements.	MSTIDs Characteristics Seismic response
8. AATR Indicator Analyze TEC data over specific region and it is mostly sensitive to ionospheric perturbations at different time scales	<u>Input:</u> slant TEC parameters. <u>Output:</u> the Along Arc STEC Rate, metric to characterize the ionosphere operational conditions of EGNOS.	TEC rate	Warning of ionospheric activity.	Warning about the availability in SBAS systems
9. Ionospheric background conditions Provides maps of the difference of the current electron density in respect to the running median conditions at various altitudes for the European region.	<u>Input:</u> the electron density distribution calculated with the TaD code (a) the current values at each grid point of the mapping area (Europe), (b) the running median values at each grid point of the mapping area <u>Output:</u> The difference between the current and the median values at each grid point.	3D ED grids with the corresponding running median.	Ionospheric Background Activity conditions over the area are estimated depending on the spatial coverage of median, positive and negative conditions.	Pixel maps indicating the perturbation of the electron density in respect to median conditions in color codes. The maps are calculated at the altitudes of 200, 300, 400 and 500 km.

Identification of the most important TID drivers and additional parameters required to be exploited for the development of the warning system are provided in TechTIDE Deliverable D3.2 [RD-3]. Classification of the TID activity for the respective methods of detection are provided in TechTIDE Deliverable D3.5 [RD-4] and summarized below in sections 3.1-3.8 jointly with the final products provided by TID identification codes in TechTIDE. Description of improvements of the TID identification methods since its first release are also provided in the following sections that were driven by users' recommendations received in the TechTIDE workshops [AD-1] and by WP5 results [RD-5].

3.1. HF-TID

HF-TID is sensitive to the quasi-periodic variations of the HF radio signal recorded on an oblique Digisonde-to-Digisonde (D2D) links. Once such quasi-periodic signal behavior is detected, HF-TID uses the observed signal to infer properties of the TID wave responsible for the variation. This method provides TID Period, Phase Velocity, Direction of propagation, Wavelength, and Amplitude.

The TID wave amplitude A_N is one of such HF-TID derived properties, readily available for categorization and presentation to the user. A_N is defined formally under assumption of a simple TID model in which, for any particular fixed altitude z_0 in the ionosphere, TID is a sinusoidal perturbation of the background density $N_0(x, y, z_0, t)$ in time t and horizontal plane (x, y) :

$$N(x, y, z_0, t) = N_0(x, y, z_0, t) \left[1 + A_n(z_0) \cos \left(\Omega t - \frac{2\pi}{\Lambda} \vec{r} \right) \right] \quad (1)$$

In addition to the TID wave amplitude $A_N(z_0)$, HF-TID method determines the angular frequency Ω , the wavelength Λ , and the direction of propagation of the TID in the horizontal plane, Θ :

$$\vec{r} = x \cos \Theta + y \sin \Theta \quad (2)$$

The perturbation amplitude $A_N(z_0)$ is an excellent candidate for a consistent and objective characterization of the TID phenomenon as evaluated by the HF-TID technique. It has a clear physical meaning and well defined minimum and maximum values. For an easier interpretation, $A_N(z_0)$ is given in %, thus ranging from 0 to 100%. We refer the reader to Deliverable D2.1 [RD-1] and Deliverable D2.2 [RD-2] for more details.

Current version of HF-TID defines five levels of LSTID activity in relation to the detected amplitude for each individual D2D radio link; **Insignificant** activity for events with $AMP < 5\%$, **Weak** for events with $5\% \leq AMP < 10\%$, **Moderate** for events with $10\% \leq AMP < 15\%$, **Strong** for events with $15\% \leq AMP < 20\%$, and **Very Strong** activity for events with $AMP \geq 20\%$. Current product of the HF-TID is shown in the Figure 1.

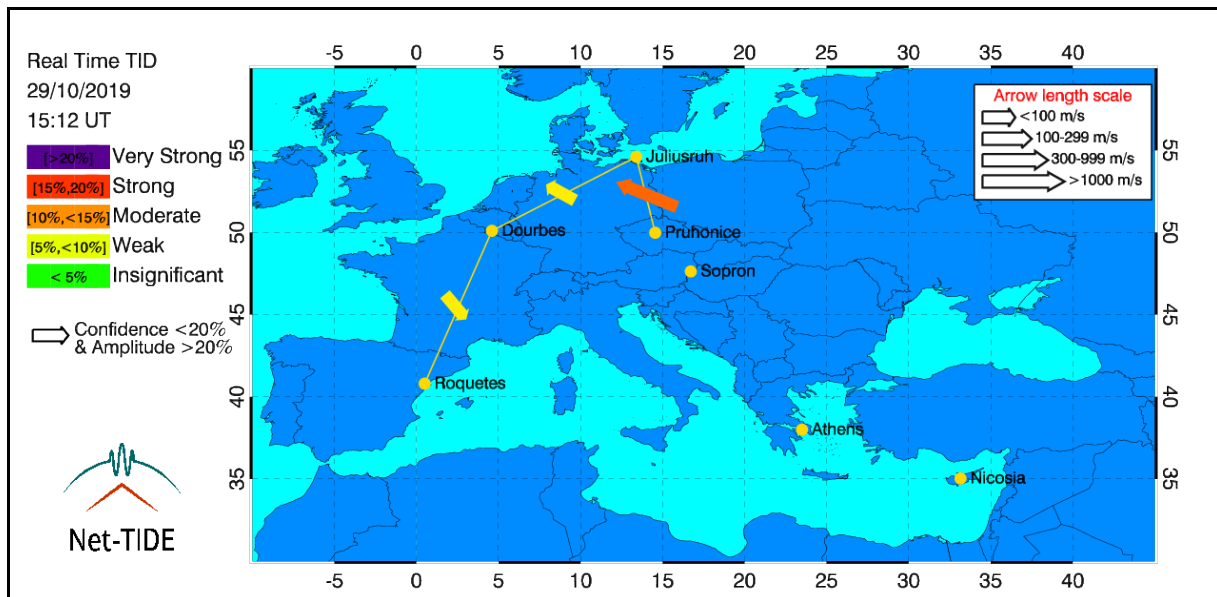


Figure 1. Example of the HF-TID product in the real-time TechTIDE warning service for a given scenario.

HF-TID method is currently under revision and in the step to define TID activity categories for presenting to each user application and to the data analysts in the TecTIDE TID activity report. The following arguments for such categorization were used to design the presentations. From experience operating HF-TID, the quiet-time level of the wave activity in the ionosphere is about 4-5%. Should there be a “**NO TID**” category introduced, with **amplitude** $\leq 5\%$. Study of the “EGU Opening Event” storm-time HF-TID data suggests that detected $A_N(z_0) = 40\%$ wave was visible in GNSS observations as a minor-to-moderate storm event. Should a “**TID**” category be introduced and positioned at that level with **amplitude** $\geq 40\%$. Then an “**UNCERTAIN**” category will be introduced for the rest of amplitude levels, $5\% < \text{amplitude} < 40\%$

3.2. HF-INT

HF-Interferometry (HF-INT) method identifies LSTIDs for the monostatic measurements of a given network of HF sensors (Ionosondes). The spatial distribution of the network should be dense enough to detect LSTID; i.e, distance between measuring sites no larger than 1000 km. The method looks for coherent oscillation activity at different measuring sites of the network and sets bounds to time intervals for which such activity occurs into a given region. HF-INT detect TID activity and provides TID Period, Amplitude, Velocity and Direction, and contribution of the TID to the total variability for a given time series.

HF-INT can only identify LSTIDs due to the geographical distribution of Digisonde sites within Europe and South Africa, whose activity are associated with auroral and geomagnetic activity, directly related to Space Weather. We refer the reader to Deliverable D2.1 [RD-1] and Deliverable D2.2 [RD-2] for more details.

The HF interferometry method uses the Maximum Usable Frequency (MUF) obtained from 10 European Digisondes and 4 Digisondes from South Africa (see Figure 2). It uses near real time data from the GIRO DIDBase Fast Chars (<http://giro.uml.edu/didbase/scaled.php>).

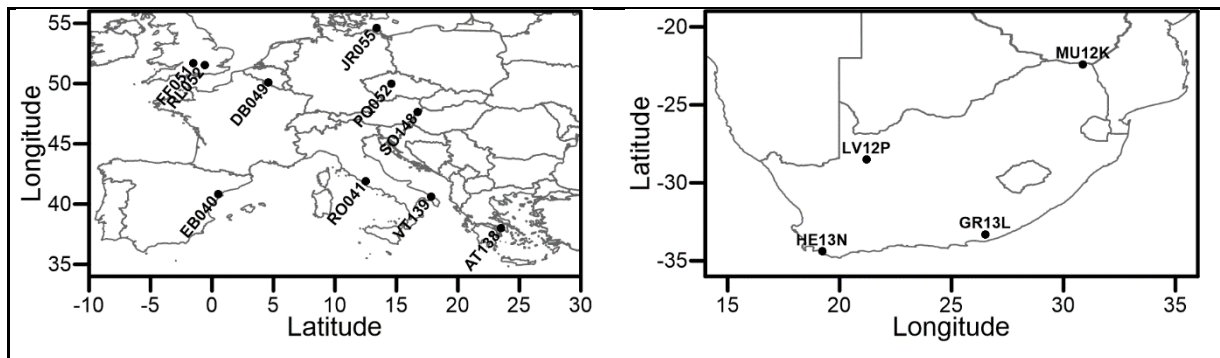


Figure 2. Geographic locations of the Digisonde stations used in the HF-INT method for Europe (left) and South Africa (right) network.

Classification of the TID activity for the HF-INT method is related to the *Spectral Energy Contribution* (SEC) of the detected TID. Thus, the larger SEC of a LSTID, the larger impact of a LSTID to the variability. The HF-INT method has been improved since its first release and the final version has adapted the levels of LSTID activity to the methods based on HF data measurements. HF-INT defines five levels of LSTID activity in relation to the detected SEC for each individual measuring sites of the network [RD-4]: Thus, HF-INT defines **Insignificant** activity for events with $SEC < 18\%$, **Weak** for events with $18\% \leq SEC < 65\%$, **Moderate** for events with $65\% \leq SEC < 80\%$, **Strong** for events with $80\% \leq SEC < 86\%$, and **Very Strong** activity for events with $SEC \geq 86\%$. Each of the above levels of LSTID activity have a given “Traffic Light” *TrL* which is a warning level indicator above each single measuring site, where $TrL=0$ means no data, $TrL=1$ means quiet or insignificant, $TrL=2$ means weak activity, $TrL=3$ means moderate activity, $TrL=4$ means strong activity and $TrL=5$ means very strong activity. HF-INT method defined also an arrow length scale according to the magnitude of the propagation velocity of the LSTIDs and direction of propagation of the disturbance above each single measuring site (Figure 3).

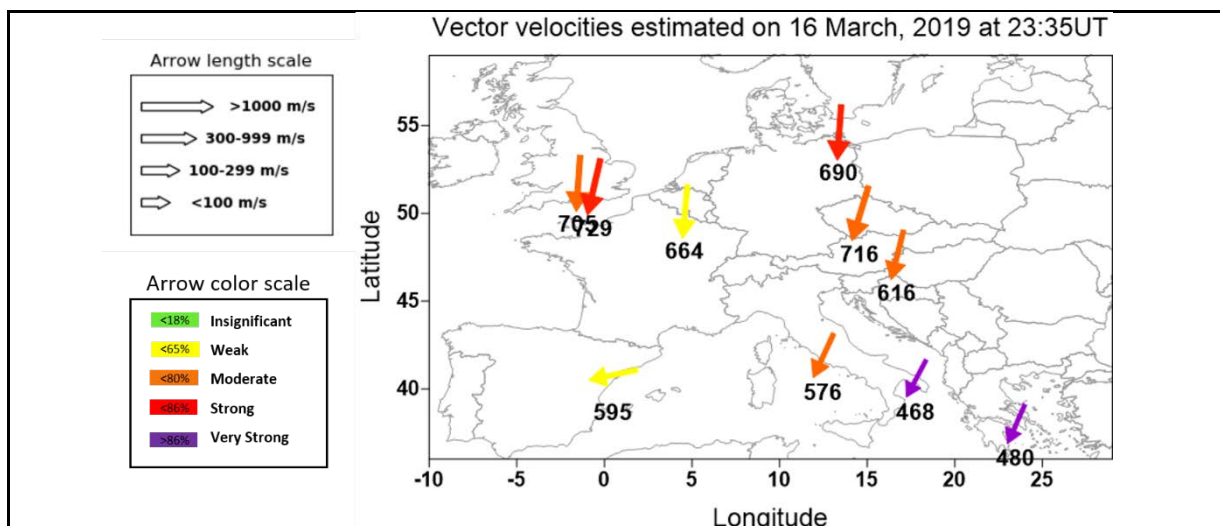


Figure 3. Example of the HF-INT product in the real-time TechTIDE warning service for a given scenario over Europe network.

An additional improvement in the HF-INT has been designed to provide a global HF-INT activity index for the European network (HF-INT_{EUx}) in addition to the local levels of LSTID activity above individual measuring sites of the network (TrL). This HF-INT activity index will apply to the TID Activity report in TechTIDE. This HF-INT activity index is obtained as the product of the average of the warning level indicators (TrL) by the ratio of the number of stations of the network reporting weak activity or larger to the total number of stations providing measurements (Equation 3).

$$HF - INT_{EUx} = \frac{N_a}{N} \cdot \frac{1}{N} \sum_{i=1}^N TrL_i, \quad (3)$$

where, N is the total number of stations providing measurements, N_a is the number of stations of the network reporting weak activity or larger, and TrL_i are the warning level indicator above each single measuring site. We made statistics (from 2014 to 2018) to establish the threshold levels to assign three different categories for the HF-INT_{EUx} (TID/UNCERTAIN/NO TID) based on the distribution of events with a given HF-INT_{EUx} or lower (Figure 4). According to the statistics, HF-INT method will provide to the TechTIDE activity report **TID** category for HF-INT_{EUx} ≥ 1.75 (the scenarios into the first decile of the distribution of the occurrence), **UNCERTAIN** category for 0.9 ≤ HF-INT_{EUx} < 1.75 (the scenarios between the first decile and the first quartile of the distribution of the occurrence), no **NO TID** category for HF-INT_{EUx} < 0.9 (the scenarios out of the first quartile of the distribution of the occurrence).

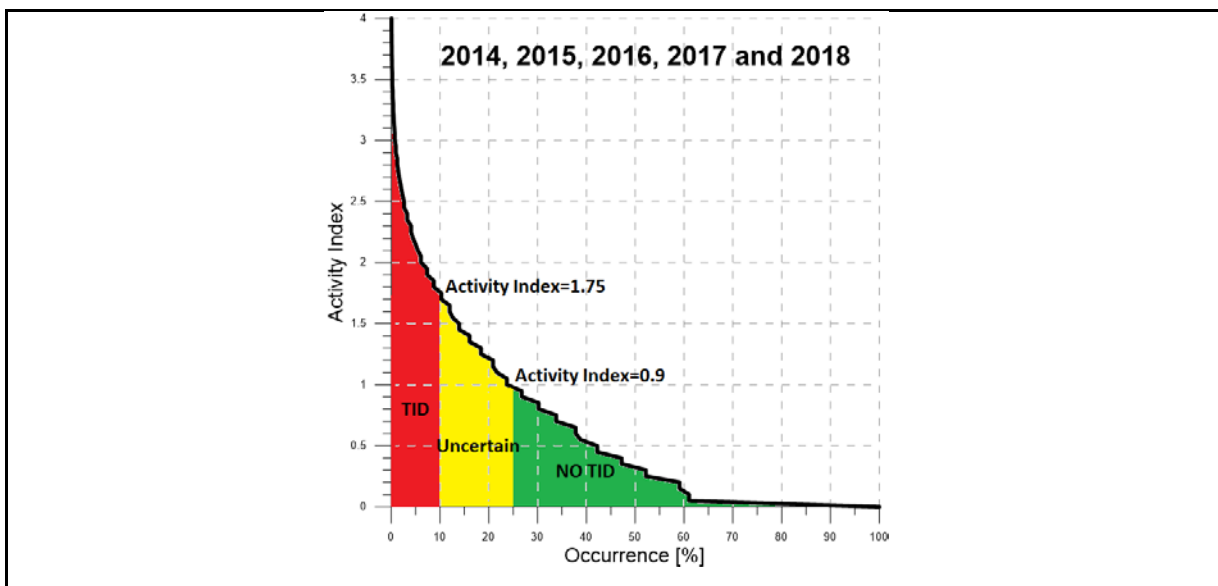


Figure 4. Distribution of the occurrence of events detected by the HF-INT method with HF-INT_{EUx} or lower.

3.3. Spatial and temporal GNSS analysis

It was shown in [RD-5] the relationship between the degradation in the performance of a NRTK service and the presence of MSTIDs, where the presence of the TIDs was characterized by means of a MSTID index (MSTID_{idx}) for each transmitter-receiver pair. Indeed, in the study, it was demonstrated that users with a single frequency receiver can achieve a significant

reduction of their positioning error by using just observations with $MSTID_{idx} < 0.01$ LI metres (being LI the geometry free combination of carrier phases, i.e. $LI=L1-L2$).

The products delivered on real-time through the TechTIDE website has been adapted to user metrics requirements, defining for the MSTID code a three level scale of $MSTID_{idx}$ for detecting disturbances [RD-4]. Thus, spatial and temporal GNSS analysis provide activity category **Low** for $MSTID_{idx} < 0.01$, **Medium** category for $0.01 \leq MSTID_{idx} < 0.02$, and **Strong** category for $MSTID_{idx} \geq 0.02$. Current product of the MSTID indicator in TechTIDE is provided in the Figure 5, a worldwide representation of the MSTID index provided in real-time to users. It is worth to mention that the location of the MSTID data points over the map in Figure 5 corresponds to the Ionospheric Pierce Point (IPP) between the GNSS station and the satellite.

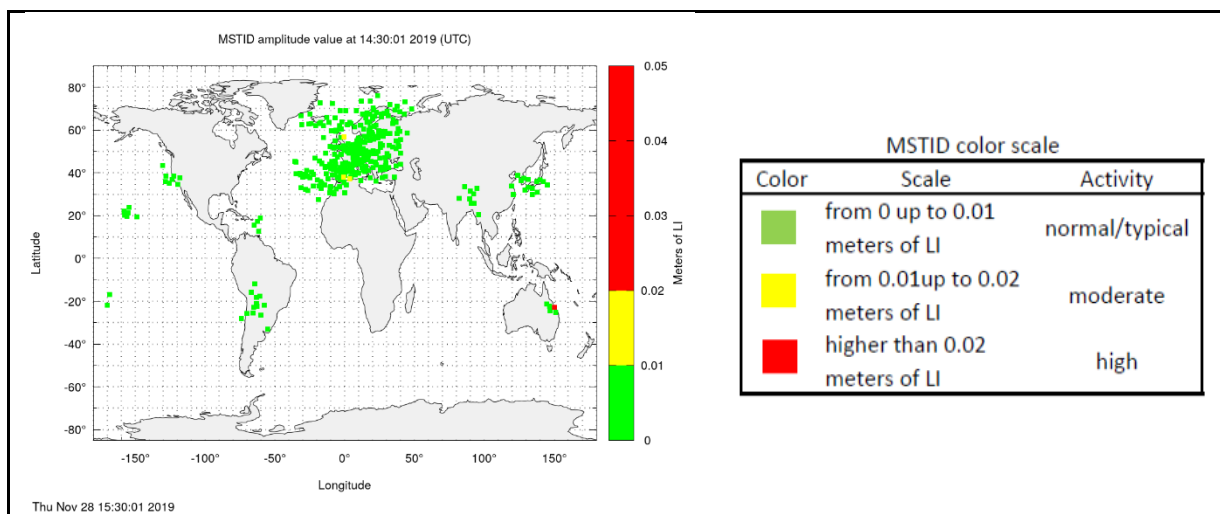


Figure 5. Example of the MSTID product in the real-time TechTIDE warning service for a given scenario.

3.4. GNSS TEC gradient

GNSS TEC gradients are not a direct measure of TIDs. Therefore, it is not applicable to classify TID occurrence based on TEC gradients. Instead, TEC gradients are considered to be a precursor for LSTID activity. Strong ionosphere-thermosphere perturbations in high-latitudes, which are generating the LSTIDs, are considered to be reflected in significant TEC gradients. Such TEC gradients associated to the generation of LSTIDs are typically observed in the Auroral region, which is over Europe in the latitudinal band between 60 and 70°N. Therefore, we used geometry TEC measurements to estimate the TEC gradients as precise as possible. The comparison between the LSTID occurrence in the detrended TEC and the TEC gradients shows that significant TEC gradients occur in high-latitudes (55-70°N) prior to the passage of LSTIDs in mid-latitudes.

For operational purposes, the fastest and most efficient approach is currently implemented, which is the estimation of TEC gradients based on TEC maps. Since the generation of TEC maps averages out steep TEC gradients, rather low thresholds have to be assumed for the indication of the probability of LSTID generation.

GNSS TEC gradient provide the following activity category for detecting disturbances [RD-4], based on the absolute value of the TEC Gradient Amplitude in high-latitudes (57-67°N)

(|Amplitude|, expressed in mm/km): **Low** category for $|Amplitude| < 1.2$, **Medium** category for $1.2 \leq |Amplitude| < 2$, and **Strong** category for $|Amplitude| \geq 2$. Current product of the GNSS TEC gradient is provided in the Figure 6.

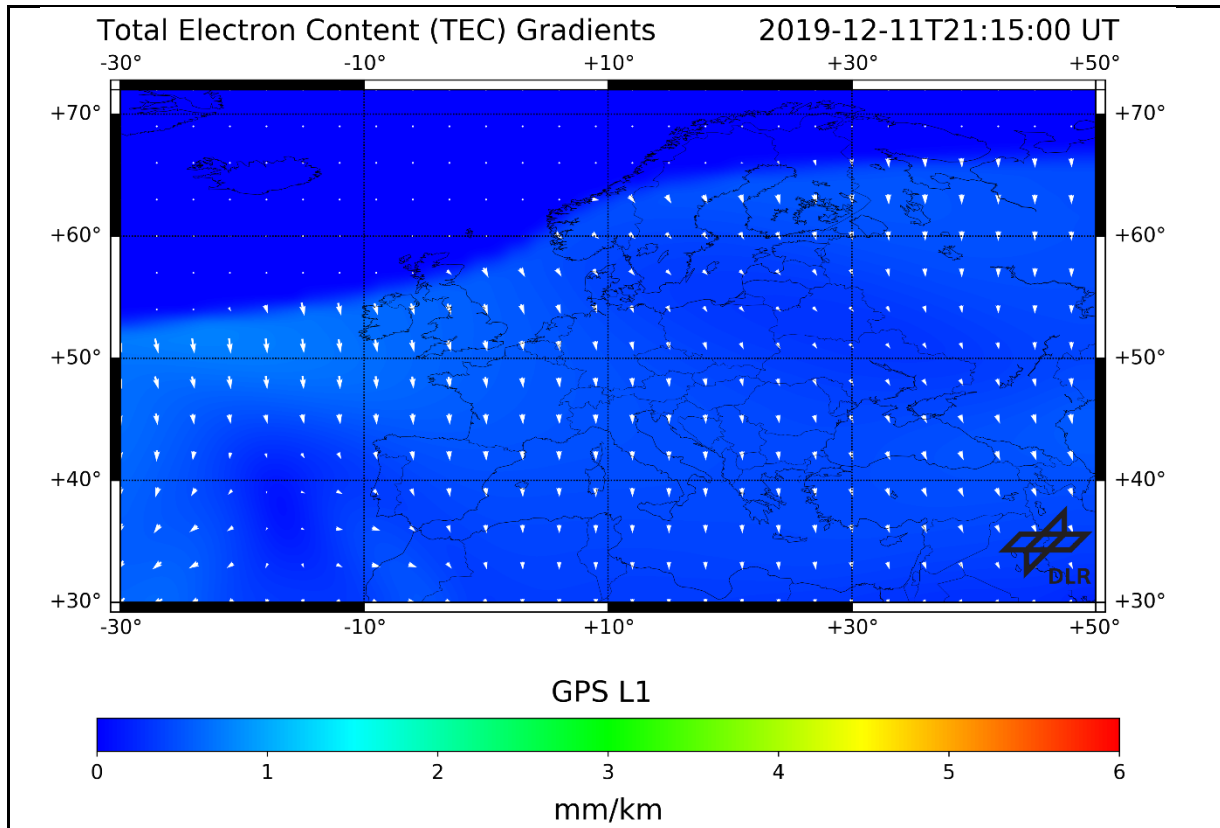


Figure 6. TEC gradients derived from IGS TEC maps in the European for a given scenario. The TEC gradients amplitude is given in mm/km.

3.5. LS TID Index

The LSTID index is the maximum value of the running relative standard deviation (RSTD%) of the electron density within 1 hour over 12 data points, at any ionospheric height from 150 to 600 km and it has been recently developed for TechTIDE. The electron density is calculated with the TaD model [RD-6]. This model provides the reconstructed electron density from the bottomside ionosphere up to the plasmasphere using as a basis the empirical model derived from the Alouette/ISIS topside sounders data, updated for the actual ionospheric and geospace conditions with the ionospheric characteristics at hmF2 (F2 critical frequency and scale height) obtained from an ionospheric sounder and with the TEC parameter at the location of the ionospheric sounder.

The correlation of the RSTD% variation with the variation of the AATR indicator calculated at high ionospheric latitudes provides quantitative criteria for the probability occurrence of the TID-related disturbances in the middle latitudes. As an example, analysis for the time period 7-12 September, where a series of geomagnetic storm effects have imposed perturbations in the ionosphere, affecting the performance of the EGNOS system is presented. Figure 7 shows the LSTID index results over Dourbes Digisonde for this interval. To assess the capability of the

LSTID index to identify LSTIDs, and since the AATR index at high latitudes is considered as a valid indicator for the LSTIDs, we use here the results from REYK, KIRU and TRDS stations (all at the auroral oval) to qualitative compare with the LSTID index results calculated for the Dourbes location. The results show a good agreement with a short time shift of the LSTID index compared to the AATR which corresponds to the travel time of TID from high to middle latitudes.

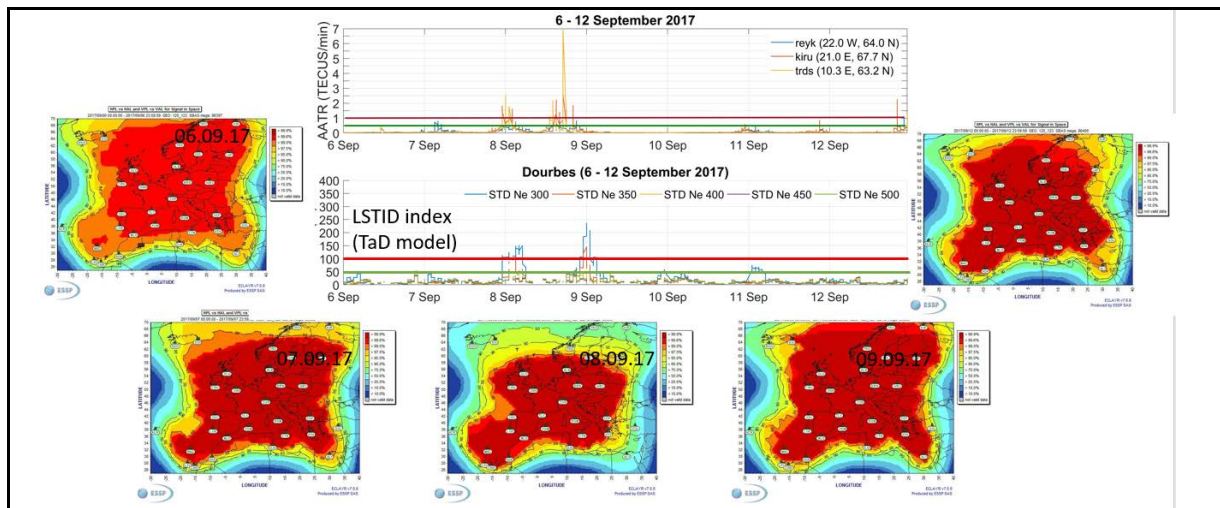


Figure 7. The LSTID index over Dourbes for the interval 6-12 September 2017 presented together with the AATR index from high altitude stations and with indicative daily maps of EGNOS availability.

The green line in the LSTID index of Figure 7 corresponds to 50% RSTD% which is put as the upper threshold for no TID activity. The red line is the threshold between uncertain conditions and TID activity conditions. Based on LSTID index and on the AATR indicator, on 7 September we have indication for unimportant to weak TID activity most of the day, until late at night when a perturbation starts. This perturbation is seen in the EGNOS availability maps at the north latitudes. On the 8 September the TID activity is more pronounced in both LSTID index and AATR indicator and in the EGNOS availability map as well.

The first results show a good agreement between LSTID index, AATR indicator and EGNOS availability. We are working to analyze more events and produce solid statistical results, which will be reported at the end of the project. The above correlation results with the following activity category of the LSTID index for detecting disturbances: for $RSTD\% < 50$ **NO TID** activity, for $50 \leq RSTD\% < 100$ **UNCERTAIN** activity, and for $RSTD\% \geq 100$ **TID** activity. Current product of the LS TID index is provided as an example in Figure 8.

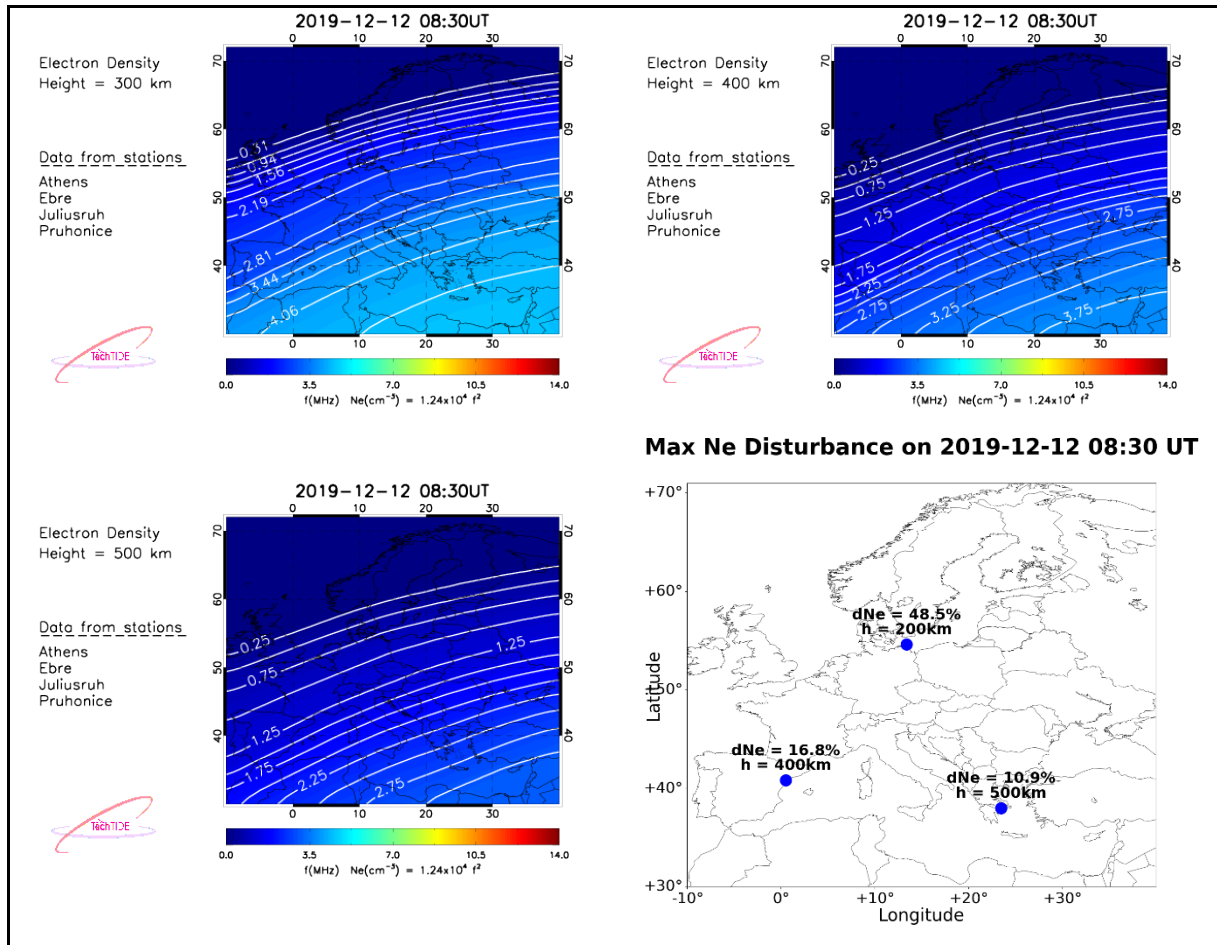


Figure 8. Examples of the electron density maps for given heights and given scenarios together with the corresponding RSTD (%) above given measuring sites (bottom-right).

3.6. HTI

The height-time-reflection intensity (HTI) algorithm enables the identification of the LSTID periodicity over each Digisonde station participating in the TechTIDE project by using the actual ionograms produced at each station. HTI has finally evolved into a real-time detection method with significant improvement modifications since its original offline specification. The final optimized version of the technique as used in the TechTIDE project exploits multiple narrow frequency bins to overcome interference causing gaps on ionogram traces. For each frequency bin at each time interval we obtain a value of the virtual height with an appropriate uncertainty (as the standard deviation) as shown in Figure 9. This is more reliable than the previous implementation of the HTI technique which relied on wide (1 MHz) frequency bins. The virtual height variation on various frequency bins is then reduced to a representative signal by removing from each the average background and a statistical fitting technique is then applied in order to examine how well a sinusoidal model describes the data (Figure 10). This approach reduces spurious variations of the virtual height and can clearly indicate when the signal is trustworthy.

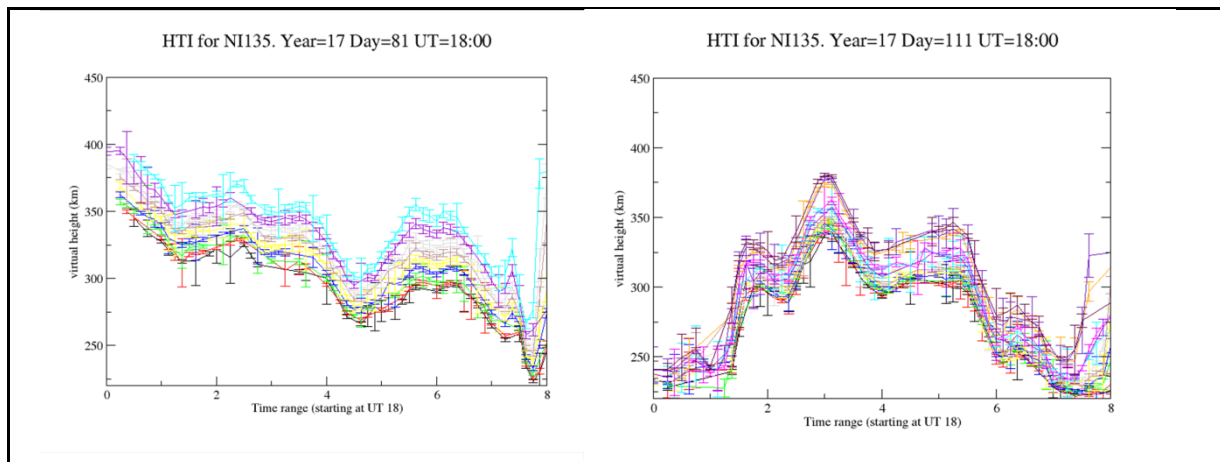


Figure 9. Example of the HTI plots for various frequency bins shown as different colors.

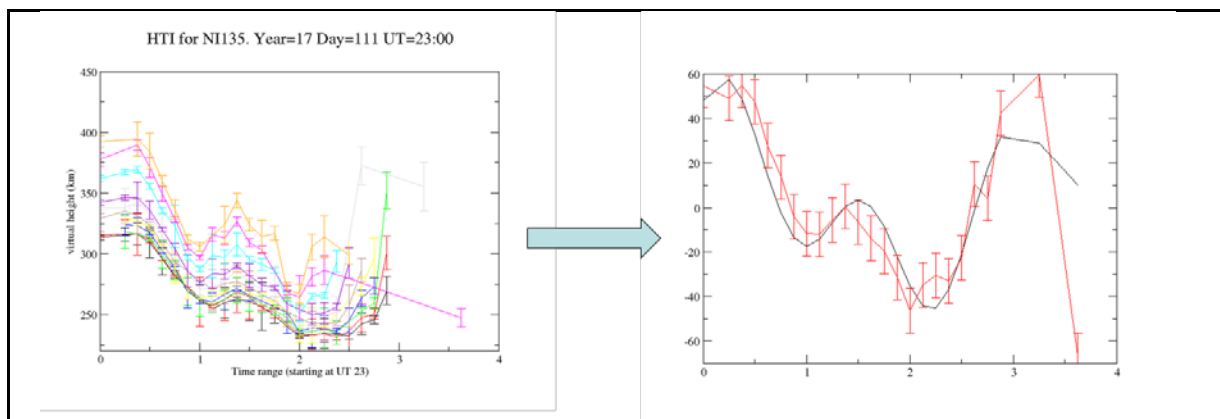


Figure 10. Statistical model fitting by combining all available frequency bins.

An additional improvement in the final real-time HTI version was the introduction of measurements of the X-mode trace in order to further enhance the overall reliability of the HTI methodology. This is particularly significant when the O-mode ionogram trace is not well defined (possibly due to interference). The final product of the HTI over a station (as shown in Figure 11) outputs the analysis results from independently processing O (black rectangles) and O and X traces (white rectangles). In this way we can identify coincidence of the two independent results which underlines the validity of the calculated periodicity.

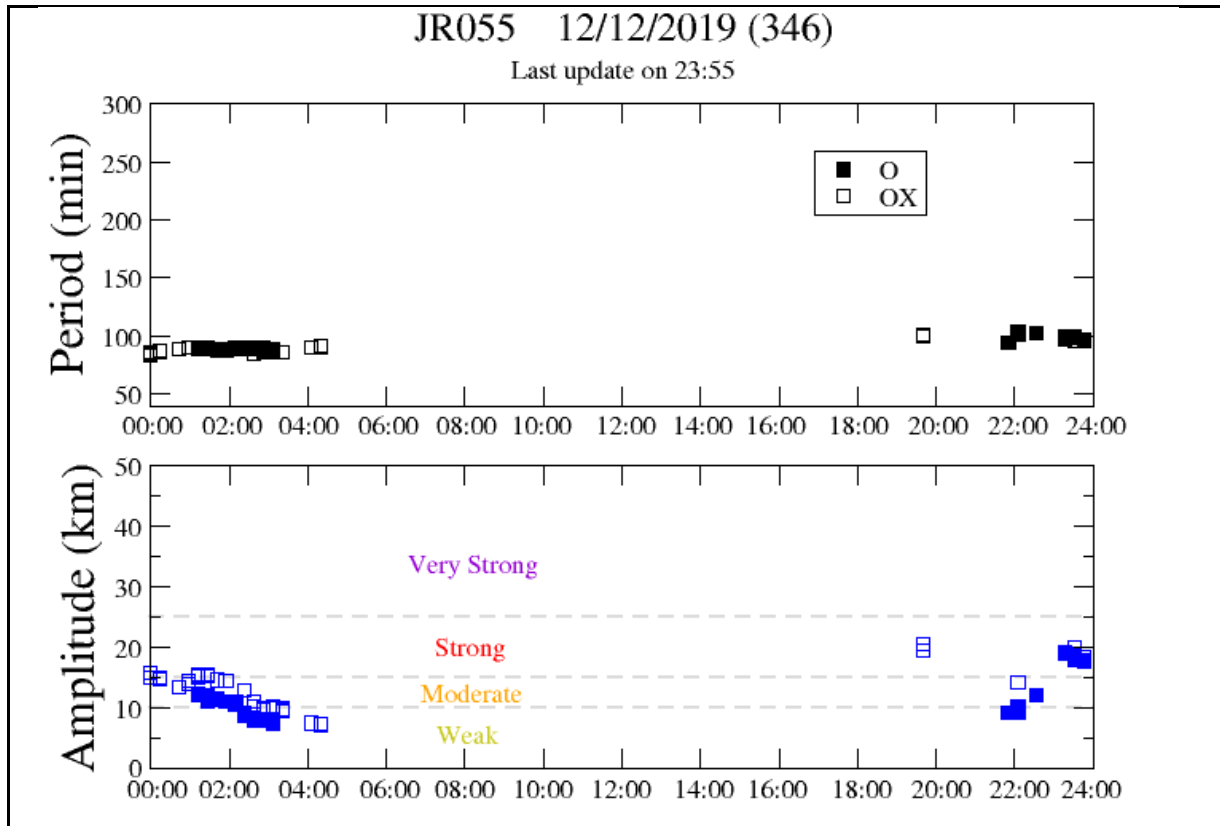


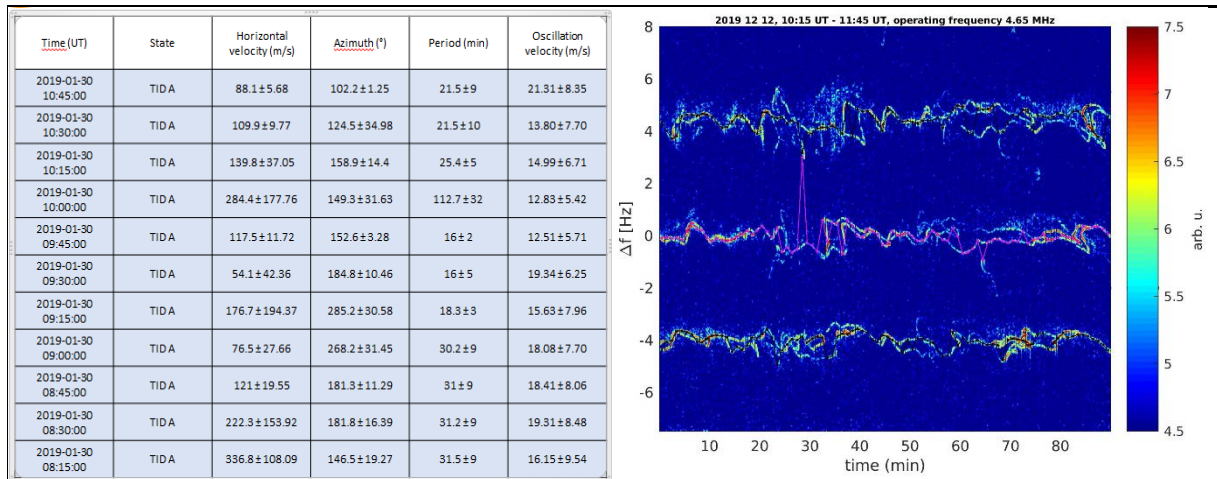
Figure 11. Daily HTI output over Juliusruh station for 12/12/2019.

3.7. CDSS-MSTID

The Czech ionospheric CDSS-MSTID method consisting of five well-spaced local networks demonstrates broad possibilities of monitoring and investigation of atmospheric gravity wave (AGW) activity related to different sources and their ionospheric signatures (e.g., ionospheric infrasound, MSTIDs). Experience and analysis provide evidence that AGWs of different periods and originated from different sources are practically permanently present in the Earth's atmosphere. Continuous Doppler sounding system (CDSS) provides direct Doppler shift measurements (Δf , expressed in Hz) of ionospherically reflected radio signals to detect MSTIDs and provides TID Period, Amplitude (AMP) and Phase of the Doppler measurements [RD-1]. CDSS-MSTID method uses these magnitudes to obtain period, amplitude, phase velocity and direction of wave propagation of MSTIDs. Based on about 15 years-long experience in CDSS measurements and expertise of wave effects on ionospheric variability allow us to define the following categories for detecting MSTID disturbances by the CDSS-MSTID method in TechTIDE [RD-4]: **Insignificant** MSTID activity for $\Delta f < 0.06$ Hz, **Moderate** MSTID activity for $0.06 < \Delta f < 0.12$, and **Strong** MSTID activity for $\Delta f > 0.12$ Hz. Horizontal propagation velocity obtained from the measurements is attached to single levels: 1st level < 100 m/sec; 2nd level: 100 - 199 m/sec; 3rd level: 200 - 350 m/sec; 4th level: > 350 m/sec.

Latest parameters/characteristics of the wave activity over the Czech Republic, as it is shown in the Table 5, could be obtained via the website <http://tid.ufa.cas.cz/>.

Table 5. Information on the parameters/characteristics of the atmospheric wave activity as it is provided on the IAP CDSS website. Spectrogram on the left is visualization of the Doppler shift product as provided in the TechTIDE warning system for a given scenario.



3.8. AATR indicator

As it can be seen in [RD-5] or in [RD-7], the Along the Arc TEC Rate (AATR measured in TECUs/min) can be used for defining ionospheric activity linked to the performance degradation of the EGNOS performance. These studies establish a threshold of around 0.5 TECUs/min for moderate activity and around 1.0 TECUs/min for high ionospheric activity.

The products delivered on real-time through the TechTIDE website has been adapted to user metrics requirements, defining for the AATR code a three level scale for assessing disturbances [RD-4]. Thus, AATR indicator provide activity **Low** category for $AATR < 0.5$, **Medium** category for $0.5 \leq AATR < 1$, and **Strong** category for $AATR \geq 1$. Current product of the AATR indicator in TechTIDE is provided in the Figure 12, a worldwide representation of the AATR indicator provided in real-time to users.

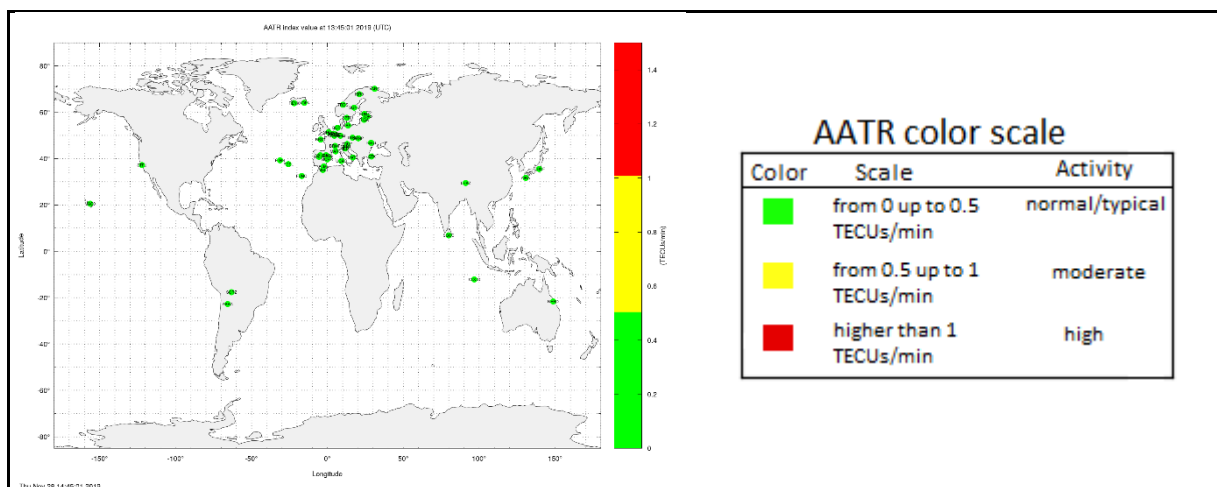


Figure 12. Example of the AATR product in the real-time TechTIDE warning service for a given scenario.

3.9. Ionospheric Background Conditions

This method evaluates as main parameter the deviation of the current electron density map from the running median electron density map. The method can be used for the identification of the background conditions (i.e. negative or positive storm events) and assess the possibility to detect ionospheric disturbances. For periods of very low background electron density, the possibility to detect TIDs is small because the amplitude of TID perturbation is directly proportional to the background electron density [RD-8]. Classification of the activity and their corresponding categories are derived by comparing the current deviation (dN_e) of the electron density from its median from the standard deviation (1σ), at each point of the grid of the map and at different altitudes covering the range from 200km to 500 km, applying a color code as follows [RD-4]: **Positive effect** for $dN_e > 1\sigma$ (Red), **Median conditions** for $|dN_e| < 1\sigma$ (Green), and **Negative effect** for $dN_e < -1\sigma$ (Blue). In addition, Ionospheric Background Activity conditions over the whole region is specified according to the following criteria:

- Median conditions are dominating: Green points > 80%
- Positive conditions are dominating : Red points > 80%
- Negative conditions are dominating : Blue points > 80%
- Conditions tend to be disturbed: positive and negative points > median points
- Conditions tend to be median: positive and negative points < median points

Current product of the Ionospheric Background Conditions in TechTIDE is provided in the examples of Figure 13. Note that the area covered by Digisonde observations is delimited in latitude and longitude by the four stations at its edges, Chilton, Ebro, Athens and Juliusruh. This area includes the 80% of the mapped region. That is why the 80% percentage is critical to characterize conditions over Europe.

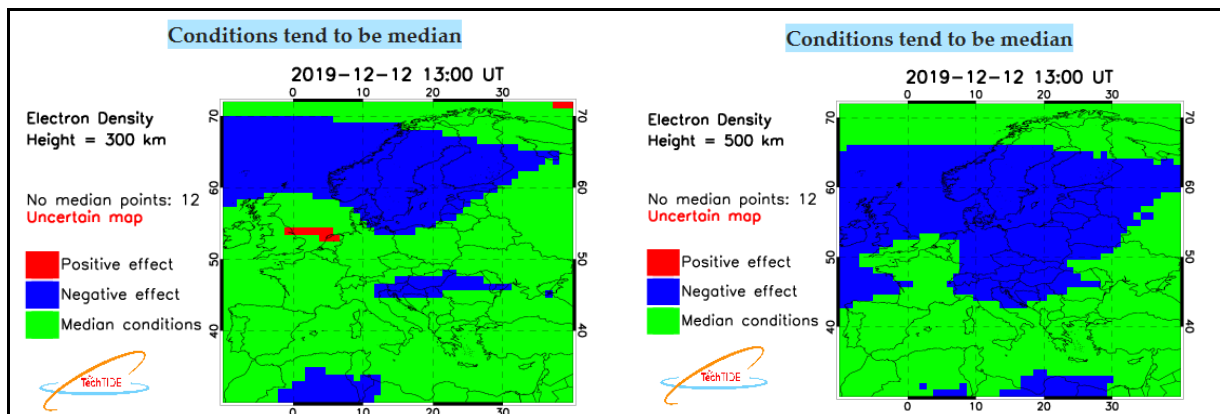


Figure 13. Maps of the residuals of the current electron density in respect to median conditions with color scales in respect to positive and negative effect. The Maps are calculated at 200km, 300km, 400km and 500 km. This example shows only the map at 200km (left) and 400km (right).

3.10. Classification of the detection products and its categories for disturbance activity

The nine products discussed above, Table 4, related to the eight methodologies operating in TechTIDE ([RD-1], [RD-2]) can be grouped into three classes [RD-4]:

- a. **Disturbance Indicators** of the ionosphere: AATR, GNSS TEC Gradient, and Background Activity Maps.
- b. **LSTID detection** methods: HF-TID, HF-INT, LSTID index, and HTI.
- c. **MSTID detection methods**: MSTID index and CDSS MSTID.

Note that **HF-TID**, **HF-INT**, and **HTI** have been grouped into the **LSTID detection** class. However, these methods can afford to detect MSTIDs if data-sampling and network topology of the sensors would be dense enough.

According to the above specifications, the classification of the methods and products in TechTIDE, with their respective levels of the disturbance activity is summarized in Table 6, Table 7, and Table 8.

Table 6. Levels of the disturbance activity for the **Disturbance Indicators** in TechTIDE.

Method	Product	Characteristic/Parameter: Levels
GNSS TEC Gradient	<u>TEC gradient map</u> : Absolute value of the gradient (Amplitude) expressed in mm/km	<u> TEC Gradient Amplitude in high-latitudes (57-67°N) </u> : [< 1.2] Low [$1.2, < 2$] Medium [> 2] Strong
AATR Indicator	<u>Activity Index</u> : AATR expressed in TECU/min	<u>AATR</u> : [< 0.5] Low [$0.5, < 1$] Medium [> 1] Strong
Ionospheric Background Conditions Indicator	<u>Detection of background ionospheric activity including positive and negative ionospheric storm effects</u> Color coded maps of the deviation of the current electron density in respect with median electron density. <ul style="list-style-type: none"> ▪ $dNe < 1\sigma$ median conditions (green) ▪ $dNe > 1\sigma$ positive (red) ▪ $dNe < -1\sigma$ negative (blue) 	<u>Ionospheric Background Activity conditions Characteristics</u> : <ul style="list-style-type: none"> ▪ Median conditions are dominating: Green points $> 80\%$ ▪ Positive conditions are dominating : Red points $> 80\%$ ▪ Negative conditions are dominating : Blue points $> 80\%$ ▪ Conditions tend to be disturbed: positive and negative points $>$ median points ▪ Conditions tend to be median: positive and negative points $<$ median points

Table 7. Levels of the disturbance activity for the **LSTID detection** of TechTIDE.

Method	Product	Characteristic/Parameter: Levels
HF-TID	<u>Detections of TID:</u> Period, Phase Velocity, Direction of propagation, Wavelength, and Amplitude (expressed as % of the perturbation in respect to the ambient electron density)	<u>Amplitude:</u> [$<5\%$] Insignificant [5% , $<10\%$] Weak [10% , $<15\%$] Moderate [15% , $<20\%$] Strong [$>20\%$] Very strong <u>Velocity:</u> 1st level <100 m/sec 2nd level: $100 - 299$ m/sec 3rd level: $300 - 999$ m/sec 4th level: >1000 m/sec <u>Azimuth:</u> TBD
HF-INT	<u>Detections of LSTID:</u> Period, Spectral Energy Contribution (SEC), Velocity, Direction of propagation	<u>SEC:</u> [$<18\%$] Insignificant [18% , <65] Weak [65% , $<80\%$] Moderate [80% , $<86\%$] Strong [$>86\%$] Very Strong <u>Velocity:</u> 1st level <100 m/sec 2nd level: $100 - 299$ m/sec 3rd level: $300 - 999$ m/sec 4th level: >1000 m/sec <u>Azimuth:</u> TBD
LSTID index	<u>Detection of LSTID:</u> Perturbation in the local values of the electron density (RSD%) at specific altitudes (from 200 to 500 km) and specific geographic locations.	<u>RSD:</u> <100 LSTID index=0; No TID $100 < RSD < 300$ LSTID index=1; Uncertain Conditions $RSD > 300$ LSTID index=2; TID
HTI	<u>Detection of LSTID:</u> Period and virtual height amplitude of LSTID over each Digisonde station.	<u>Virtual height amplitude:</u> [<5 km] Insignificant [5 , < 10 km] Weak [10 , < 15 km] Moderate [15 , < 20 km] Strong [> 20 km] Very strong

Table 8. Levels of the disturbance activity for the **MSTID detection** of TechTIDE.

Method	Product	Characteristic/Parameter: Levels
MSTID index	<u>Activity Index:</u> MSTID_idx expressed in m of LI (1 TECU=0.105 m of LI)	<u>MSTID_{idx}:</u> [<0.1] Low [0.1 , <0.2] Medium [>0.2] Strong NRTK: [<0.01] Quiet

Method	Product	Characteristic/Parameter: Levels
CDSS-MSTID	<u>Detections of MSTID:</u> Period, Amplitude, Phase velocity, Direction of propagation	<u>Doppler shift:</u> [<0,06] Insignificant [0,06, <0,12] Moderate [0,12, <018] Strong <u>Velocity:</u> 1st level <100 m/sec 2nd level: 100 - 199 m/sec 3rd level: 200 - 350 m/sec 4rth level: >350 m/sec <u>Azimuth:</u> TBD <u>Coherency:</u> 0-1

The different methodologies furnish the information of the [TechTIDE warning system](#) [RD-9], which is also grouped into three classes as **Disturbance Indicators**, **LSTID Detection**, and **MSTID detection** products. Moreover, the **categories** of disturbance for the different products have been developed according to user needs as provided in the two users workshops held in Neusterlitz, Germany, on May 2019 (1st TechTIDE User Workshop; MS#9 [AD-1]) and in Prague, Czech Republic, on October 2019 (1st TechTIDE User Workshop; MS#10 [AD-1]). These provides three category standards for the LSTID detection methods; **TID**, **UNCERTAIN**, and **No TID**; three standards for the MSTID detection methods and for the TEC gradients and AATR index Disturbance Indicators; **Low**, **Medium**, and **Strong**; and three standards, **Positive**, **Median**, and **Negative**, for the Ionospheric Background Conditions. Table 9, Table 10, and Table 11 provide the **categories** of disturbance for Disturbance Indicators, LSTID detection, and MSTID detection methods respectively.

Table 9. Categories of the disturbance for the **Disturbance Indicators**.

Method	Category	Results
TEC gradients	Low / Medium / Strong	Click here for details
AATR	Low / Medium / Strong	Click here for details
Ionospheric Background Conditions	Positive/Median/Negative	200km , 300km , 400km , 500km

Table 10. Categories of the disturbance for the **LSTID Detection Methods**.

Method	Category	Results
HF-TID	TID / UNCERTAIN / No TID	Click here for details
HF-INT	TID / UNCERTAIN / No TID	Click here for details
1D dEDD over Ebro	TID / UNCERTAIN / No TID	Click here for details
1D dEDD over Dourbes	TID / UNCERTAIN / No TID	Click here for details
1D dEDD over Juliusruh	TID / UNCERTAIN / No TID	Click here for details

Method	Category	Results
1D dEDD over Athens	TID / UNCERTAIN / No TID	Click here for details
1D dEDD over Hermanus	TID / UNCERTAIN / No TID	Click here for details
1D dEDD over Grahamstown	TID / UNCERTAIN / No TID	Click here for details

Table 11. Categories of the disturbance for the **MSTID Detection** Methods.

Method	Indication	Results
MSTID index	Low / Medium / Strong	Click here for details
CDSS MSTID	Insignificant/Moderate/Strong	Click here for details

4. Results of the TID methods and products in TechTIDE and TID impact on aerospace and ground systems

This section presents an evaluation of the results of the TID detection methods and products in TechTIDE to support specific systems operations. Analysis of the TID impact on aerospace and ground systems based on the above results is also provided. The analysis is done for retrospectively detected events and for real-time detected events.

4.1. Impact of TechTIDE TID detection on aerospace systems

In order to analyze the impact of TID detected by TechTIDE method/products on aerospace systems we focus first our analysis on scenarios with degrades EGNOS availability. As already mentioned above, the AATR indicator can be used for defining ionospheric activity linked to the degradation of the EGNOS performance ([RD-5], [RD-7]). As an example, Figure 14 shows the temporal evolution of the EGNOS APV-I availability at RIMS EGI (65.1N, 14.4°W) (black line) and AATR values at two IGS stations: ARG1 (61.8°N, 6.8°W) (purple line) and REYK (64.0°N, 22.0°W) (green line) from 7th to 9th September (DOY 250 to 252).

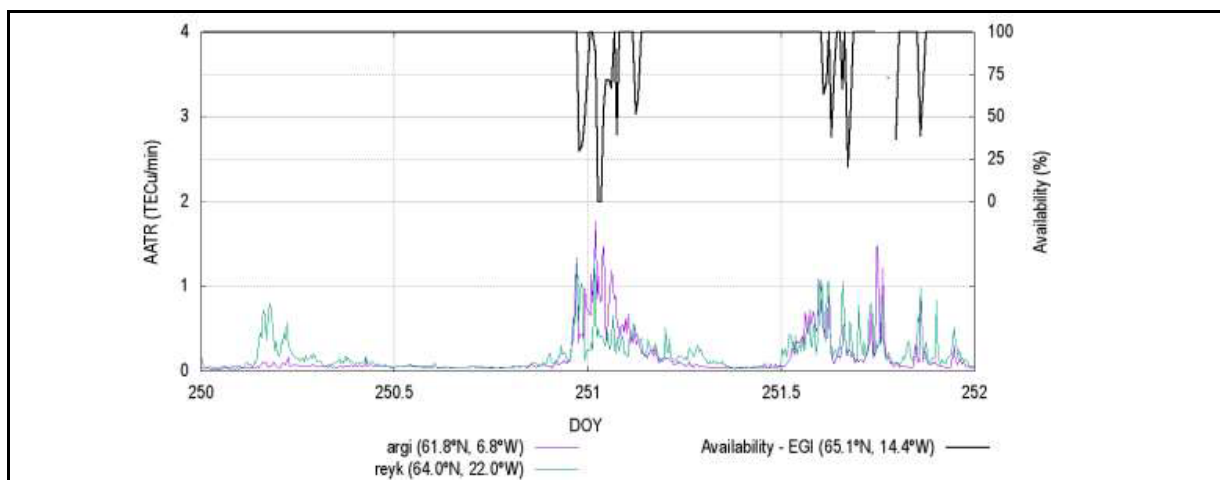


Figure 14. APV-I availability at RIMS EGI (black), AATR values at IGS station ARG1 (purple) and REYK (green) from 7th to 9th September (DOY 250 – 252). Plot gathered from [RD-5].

The analysis of this availability degradations reveals that all these degradations are linked to ionospheric activity related to series of disturbances occurred in September 2017, initiated with a solar flare on 6 September ([RD-4]).

Based on the list of scenarios were selected to identify the EGNOS APV-I availability degradation linked to ionospheric effects (see Table 2 of [RD-5]) we present the results of the TID detection methods and products to assess specific TID impact on systems operations.

HF-TID method provide also products through the online TID Explorer (<https://backends.giro.uml.edu/tidx/>). This tool was used to retrieve TID event detection data for comparison with the EGNOS APV-I service degradation data. As an example, a typical TID Explorer display is shown in the Figure 13. Color bar in the top of the Figure 15 indicates the occurrence of the EGNOS degradation (Red).

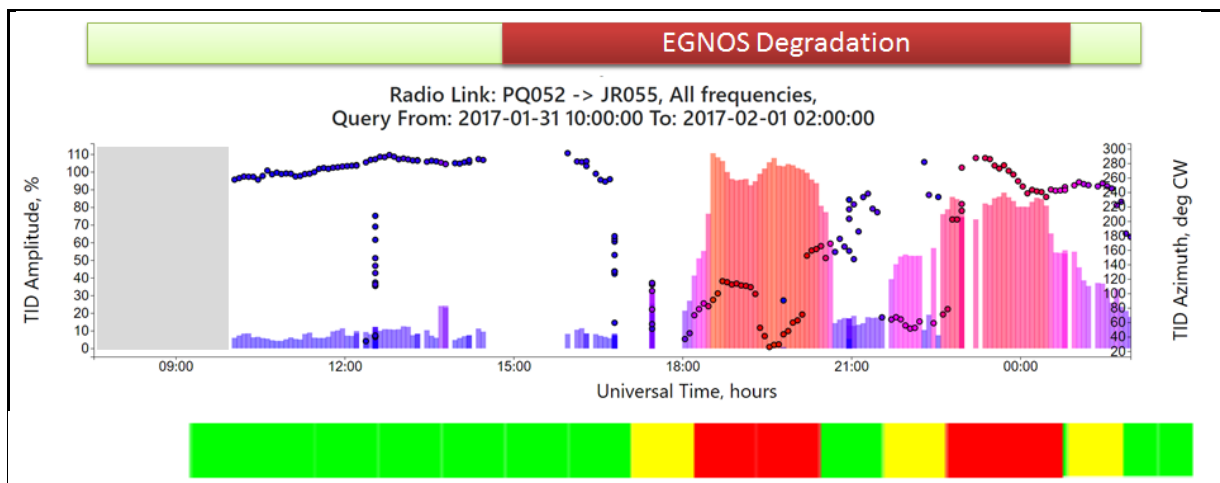


Figure 15. Example of a HF-TID event detection data for a given radio link (middle) compared with the EGNOS APV-I service degradation data (top).

The TID Explorer charts use vertical color bars to represent TID amplitude A_N (the left y-axis) and the color dots to plot the azimuth of TID propagation Θ (the right y-axis). The chart example in Figure 15 shows a very strong TID event detected over the Northern Germany between 2017-01-31 1900 UT and 2017-02-01 0100 UT. Color bar at the bottom correspond to the category introduced in section 3.1 **TID** at the level with amplitude $\geq 40\%$ (Red), **UNCERTAIN** at levels, $5\% < \text{amplitude} < 40\%$ (Yellow), and **NO TID** the level with amplitude $\leq 40\%$ (Green). Time interval shaded in gray indicates no D2D data measurements was available. The category of the disturbance represented in the bottom bar has been binned at hourly intervals for simple comparison of TID detection with the EGNOS degradation. Such a representation will be used for further analysis results.

The results of comparison for this case study reveal that TID activity as provided by HF-TID method coincides with EGNOS degradation. However there is an apparent delay on the TID detection in relation to de degradation. It should be noticed here that the above TID detection

correspond to a particular region between Germany and the Czech Republic, whereas the EGNOS degradation refer to a much broader area.

Similarly to HF-TID method, results of TID detection by HF-INT are presented in the Figure 16, where color bar in the top indicates the occurrence of the EGNOS degradation (Red). Vertical color bars in the middle plot represent the SEC (%) of the TID detection over Juliusruh (54.6N, 13.4E) whose colors are arranged according *TrL* levels introduced in section 3.2 and according to the arrows color scales shown in Figure 3. Small vertical color bars in the bottom shows the 5-min evolution of the HF-INT_{EUx} (Equation 3), which are colored according to defined categories in section 3.2 (Figure 4). Finally, the category of the disturbance represented in the bottom color bar depicts HF-INT_{EUx} averaged and binned at hourly intervals for simple comparison of TID detection with the EGNOS degradation. Such a representation will be used for further analysis results.

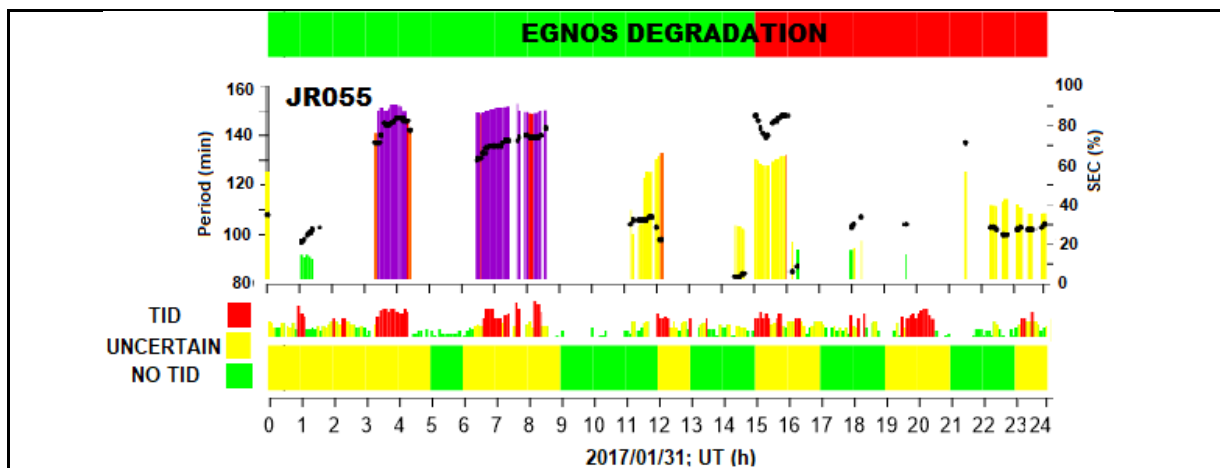


Figure 16. Example of a HF-INT event detection data for a given sensor located in Germany (middle) compared with the EGNOS APV-I service degradation data (top) and for a given scenario.

The results of comparison for this case study reveal that two TID activity events were detected by HF-INT method in the early morning hours (at 3-4, and 6-8 UT) indicating strong TID level, especially in the north part of Europe, which seems to not affect EGNOS degradation. Two additional TID activity events were detected at 15-16 UT and 19-20 UT (the later not reported in Juliusruh) that coincide with an interval of EGNOS degradation.

Following the same approach as above, we compare the disturbance activity reported by the TechTIDE methods/products that might be linked to degradation of the EGNOS performance. Figure 17 shows an example of comparison for a particular scenario. The category of the disturbance represented in the different color bar has been binned at hourly intervals for simple comparison of disturbance detection with the EGNOS degradation. We refer as EGNOS degradation (EGNOS-D) as the EGNOS APV-I 99% Availability Degraded Area, and we have defined EGNOS-D categories **Low** for $EGNOS-D \leq 5\%$ (Yellow), **Medium** for $5\% < EGNOS-D \leq 15\%$ (Orange), **Strong** for $EGNOS-D > 15\%$ (Red). The different method/products are organized according to section 3.10 as disturbance **Indicators**, **LSTID** and **MSTID** detection methods respectively. We use the three category standards described in section 3.10: **TID** (Red), **UNCERTAIN** (Yellow), and **No TID** (Green) for LSTID products; **Low** (Green), **Medium** (Yellow),

and **Strong** (Red) for the MSTID products and for the TEC gradients and AATR index Disturbance Indicators (Table 9, Table 10, and Table 11).

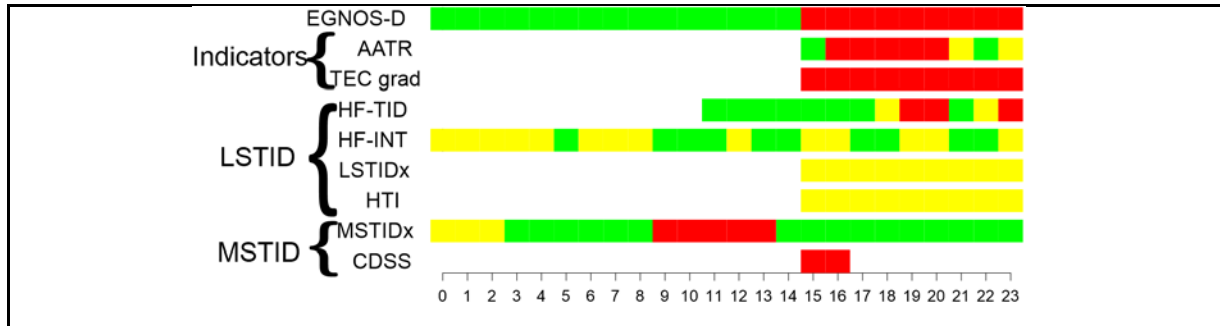


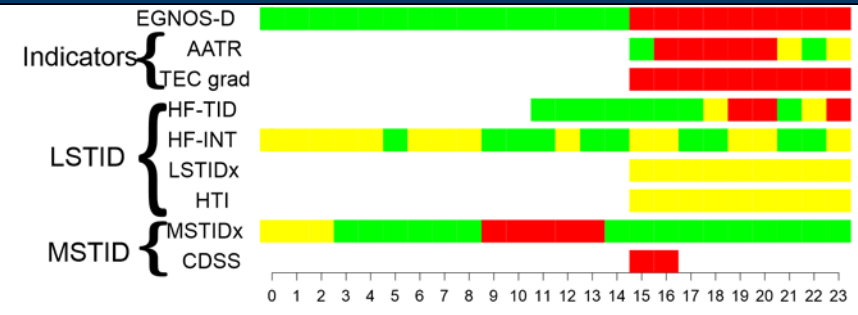
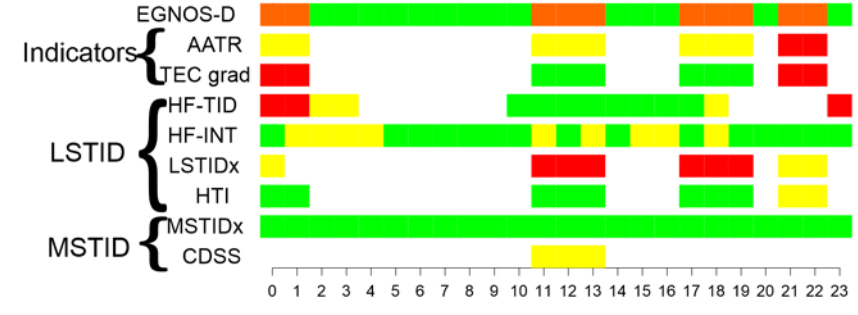
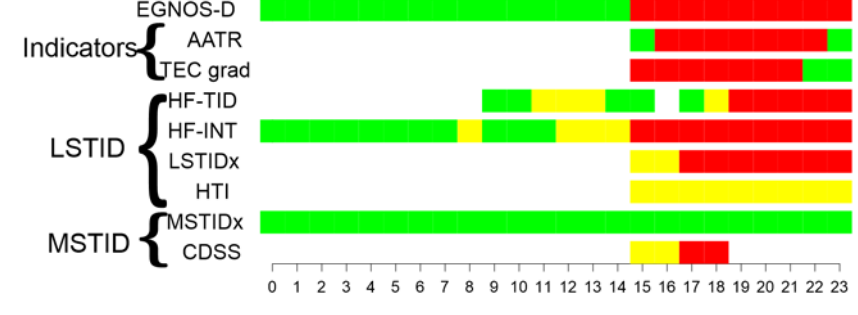
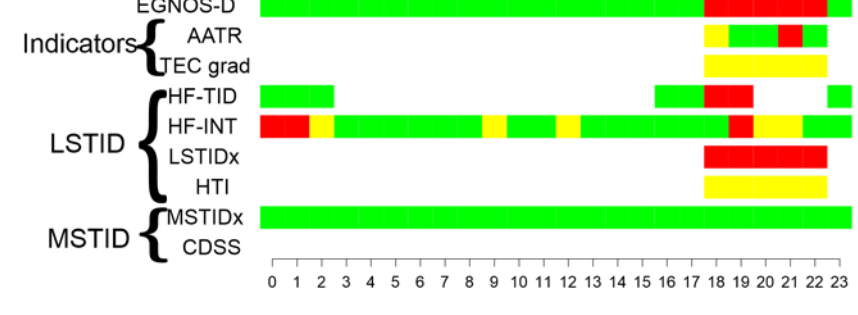
Figure 17. Comparison of the disturbance activity reported by the TechTIDE methods/products with EGNOS APV-I 99% Availability Degraded Area for 31st January 2017.

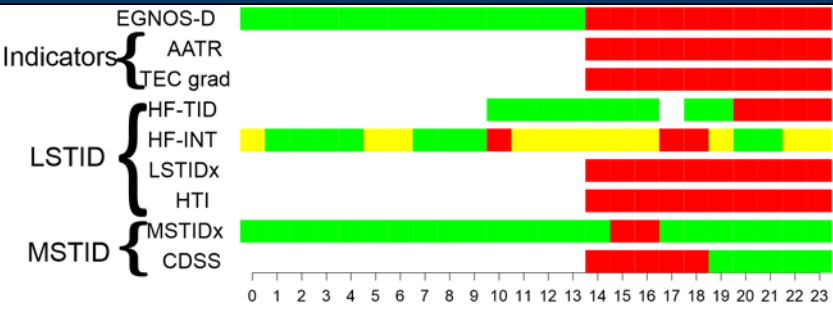
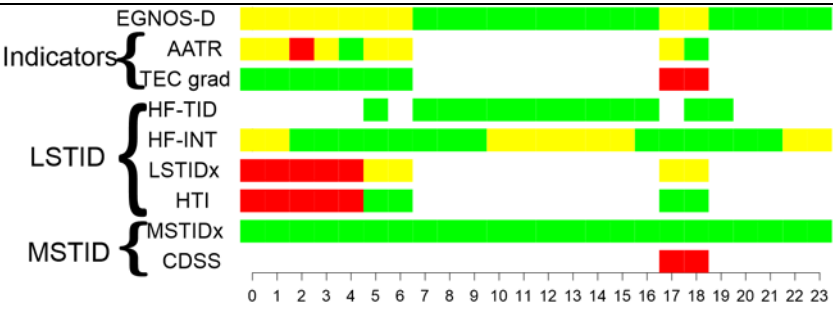
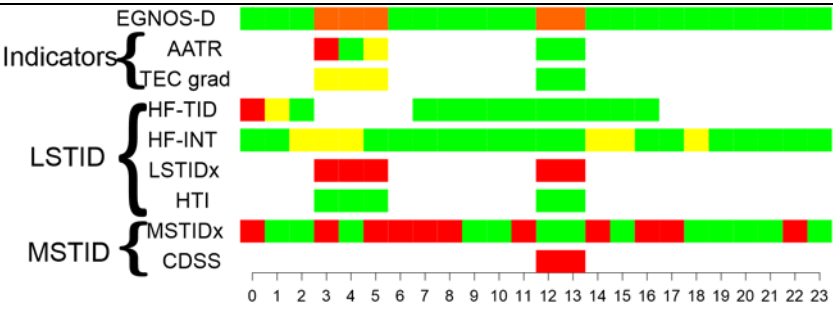
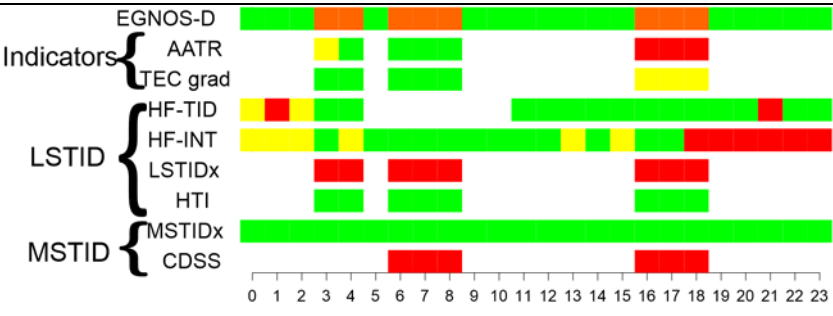
Figure 17 shows for this particular scenario a very good agreement when compare the Disturbance **Indicators** with EGNOS-D. This was expected as per [RD-5], [RD-7]. LSTID products report some TID activity when EGNOS-D is disturbed but agreement is not as good as reported for Disturbance Indicators. MSTID products reports also simultaneous or advanced activity to the EGNOS-D disturbance. Although the agreement of the activity detected by MSTID methods is not as good as for the Disturbance Indicators, it seems to be reasonable for this particular scenario.

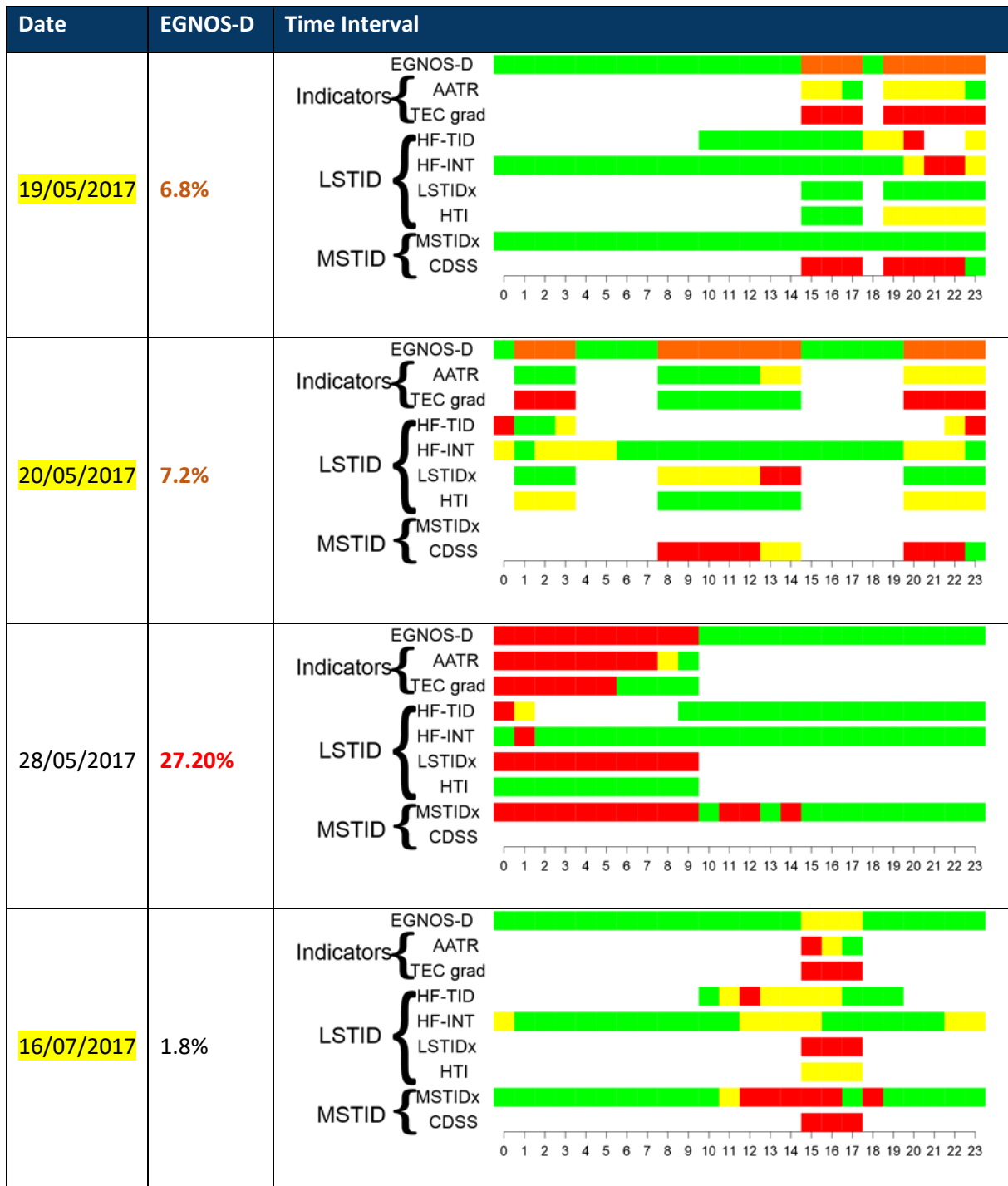
Such a kind of analysis has been done for all the scenarios reported in the Table 2 of the [RD-5] which are presented in Table 12. Color of the percentage of EGNOS-D in Table 12 are arranged as follow: Black means EGNOS-D<5%, orange means 5%≤EGNOS-D<15% and read means EGNOS-D≥15%. Degradation computed along all day where additional causes could increase the underperformance are highlighted in yellow.

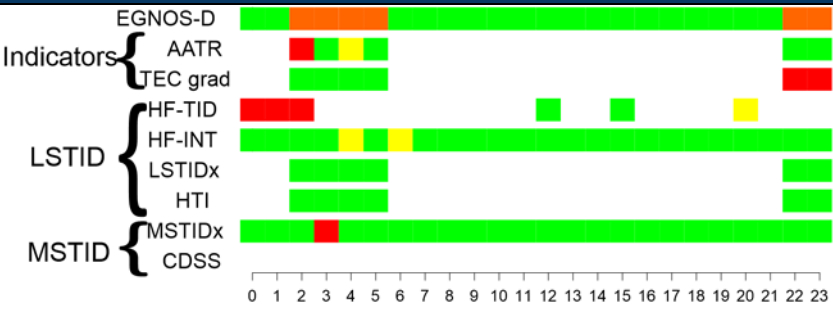
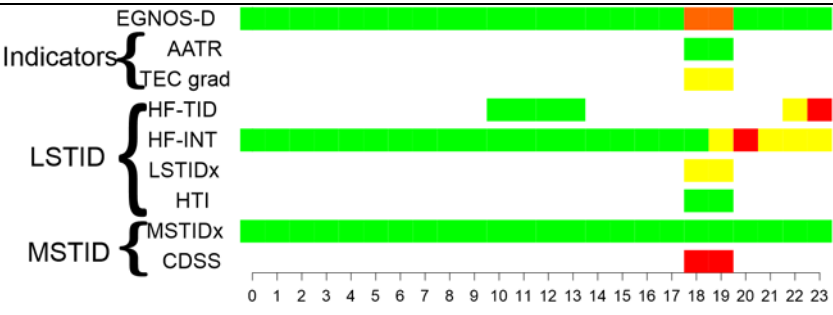
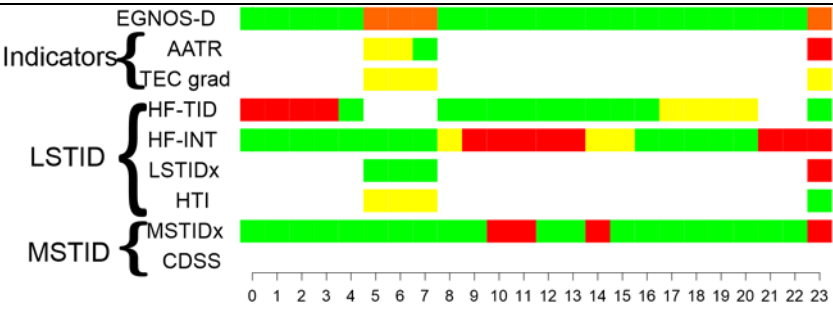
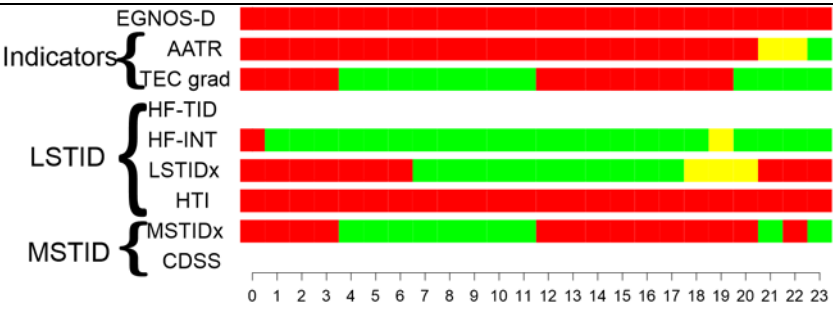
Note that HTI method provides information above 5 single stations in Europe (Section 3.6). In this sense, in Table 12, we have considered that HTI detects TID activity if 3 or more stations report some activity, uncertain if only 2 or less detects some activity and no TID for remaining cases. Concerning MSTID_x, we indicate in the Table 12 the MSITID_x for central Europe. Finally, as refers to the information of the CDSS-MSTID product, we have to consider that results are only relevant for the Czech Republic (western part) and that many of the time scenarios specified in Table 12 fit into periods when foF2<4.65 MHz; hence, no information is available using CDSS-MSTID at 4.65 MHz. In addition, concerning the results presented in Table 12, it should be noted that most of the TechTIDE methods/products report information for the time interval when EGNOS-D is degraded, and only HT-INT and MSTID_x provide full day information as EGNOS-D does.

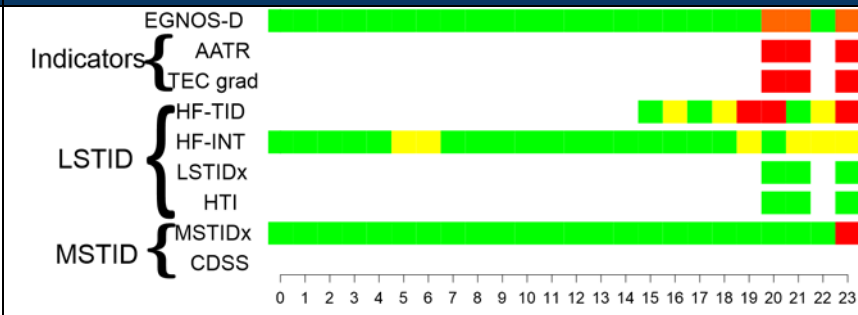
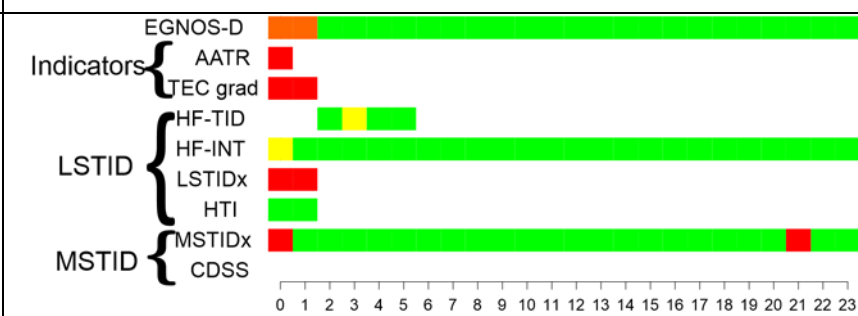
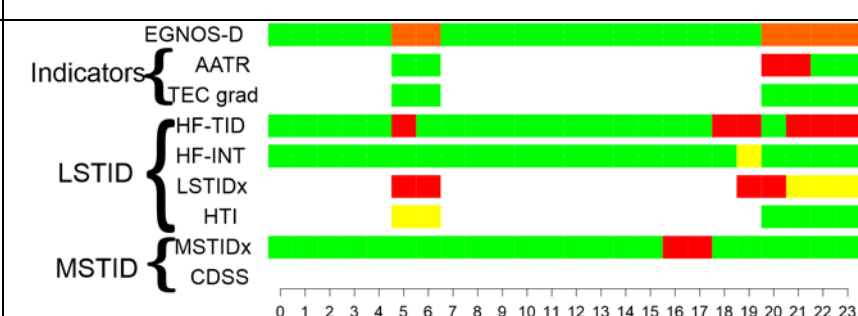
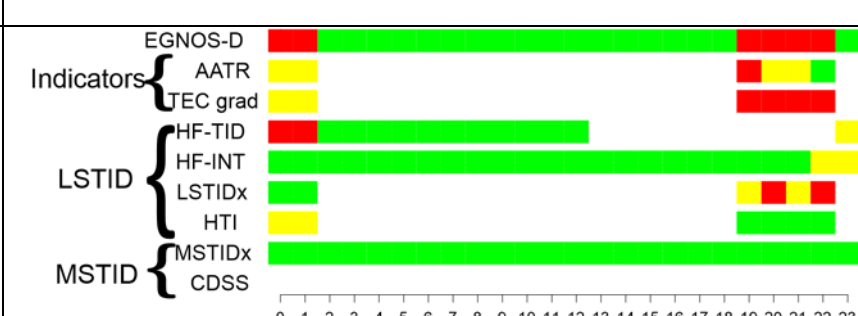
Table 12. List of scenarios analyzed comparing the EGNOS APV-I 99% Availability Degraded Area (EGNOS-D) with category of disturbances detected by the indicated TechTIDE methods/products.

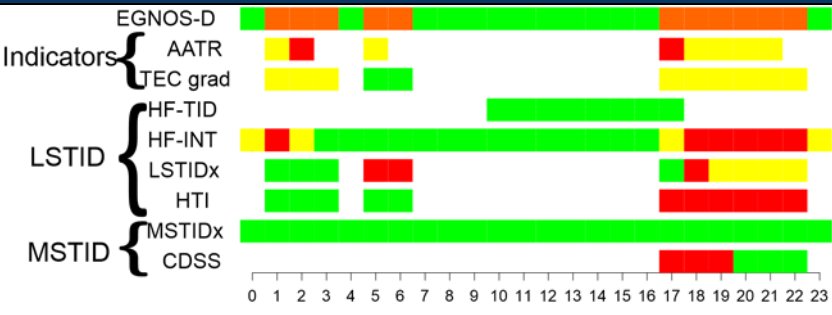
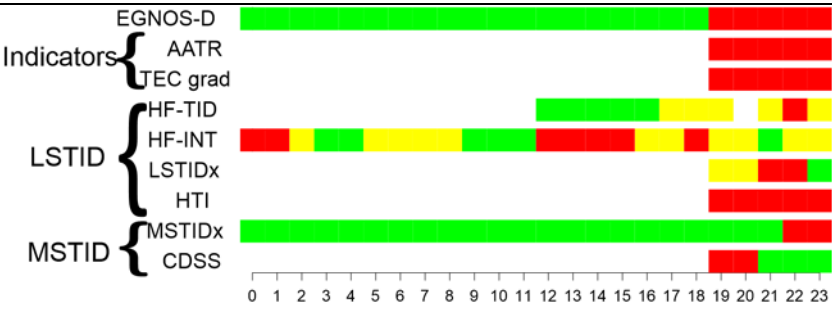
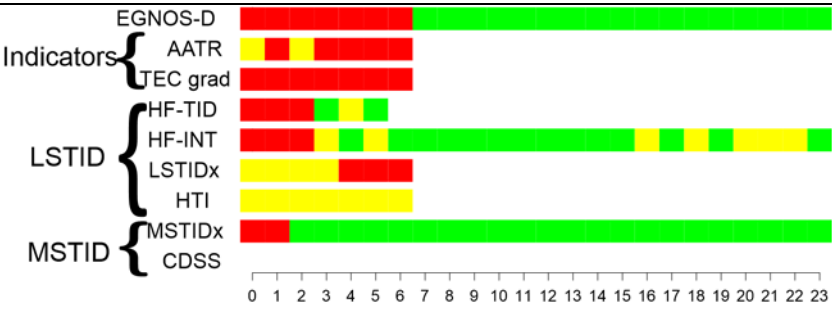
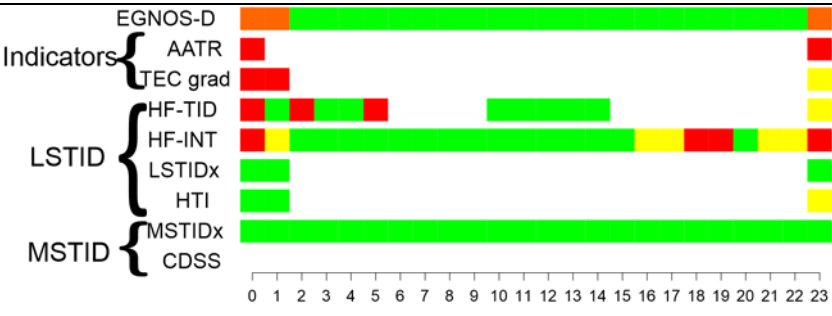
Date	EGNOS-D	Time Interval
31/01/2017	19.10%	
01/02/2017	9.5%	
01/03/2017	16.10%	
02/03/2017	21.70%	

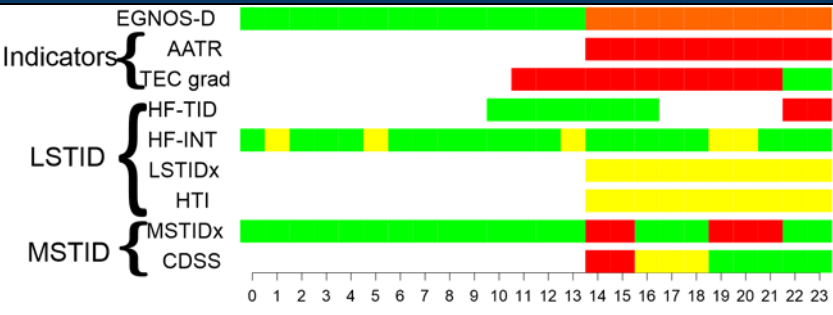
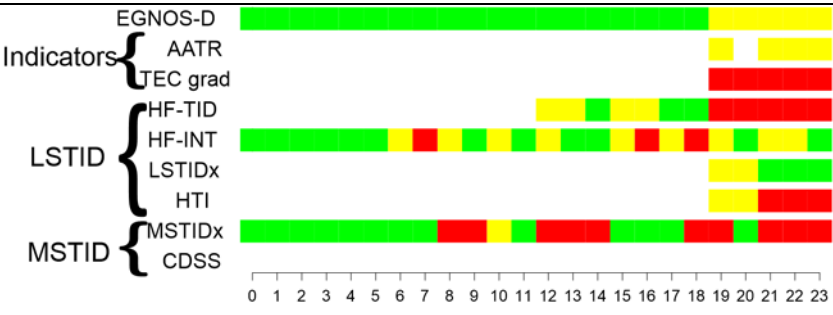
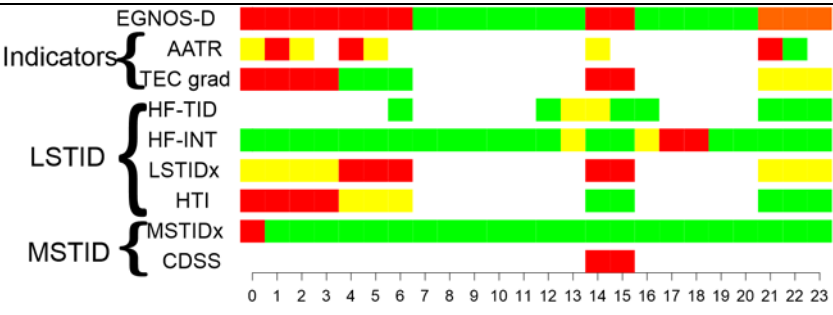
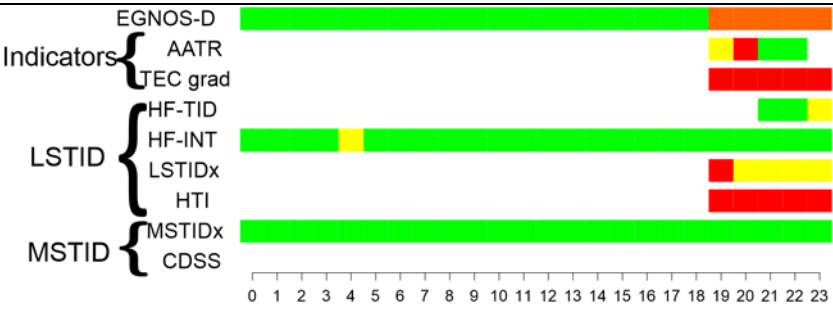
Date	EGNOS-D	Time Interval
27/03/2017	19.30%	
28/03/2017	4.1%	
20/04/2017	7.4%	
23/04/2017	7.1%	


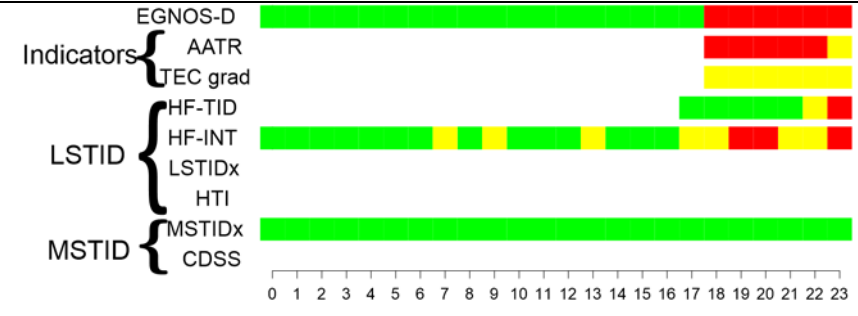
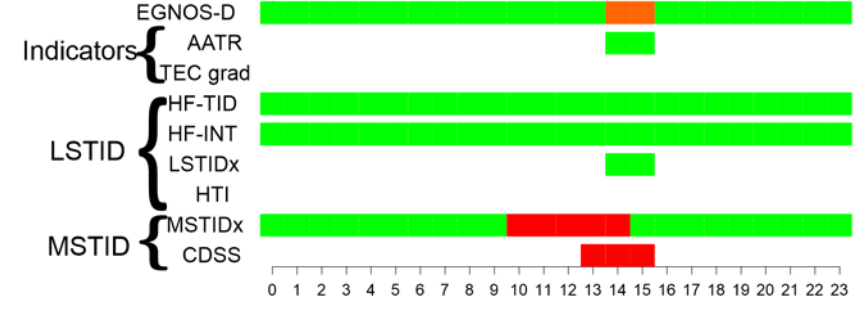


Date	EGNOS-D	Time Interval
22/08/2017	6.6%	
23/08/2017	5.9%	
07/09/2017	12.0%	
08/09/2017	36.7%	

Date	EGNOS-D	Time Interval
12/09/2017	10.9%	
13/09/2017	8.7%	
14/09/2017	6.0%	
15/09/2017	15.7%	

Date	EGNOS-D	Time Interval
16/09/2017	7.6%	 <p>EGNOS-D: 0-23 (Green)</p> <p>Indicators: AATR (0-2, 4-5, 17-18), TEC grad (0-3, 5-6, 17-22)</p> <p>LSTID: HF-TID (10-17), HF-INT (0-2, 3-17, 18-23), LSTIDx (0-3, 5-6, 17-18, 19-22), HTI (0-3, 5-6, 17-22)</p> <p>MSTID: MSTIDx (0-23), CDSS (17-18, 19-22)</p>
27/09/2017	15.4%	 <p>EGNOS-D: 0-18 (Green), 19-23 (Red)</p> <p>Indicators: AATR (19-23), TEC grad (19-23)</p> <p>LSTID: HF-TID (12-17, 18-19, 21-22, 23), HF-INT (0-2, 3-4, 5-8, 9-12, 13-15, 16-18, 19-20, 21-22, 23), LSTIDx (19-20, 21-22, 23), HTI (19-23)</p> <p>MSTID: MSTIDx (0-23), CDSS (19-20, 21-22)</p>
28/09/2017	15.4%	 <p>EGNOS-D: 0-6 (Red), 7-23 (Green)</p> <p>Indicators: AATR (0-2, 3-4, 5-6), TEC grad (0-6)</p> <p>LSTID: HF-TID (0-3, 4-5, 6), HF-INT (0-2, 3-4, 5-6, 7-16, 17-18, 19-20, 21-22, 23), LSTIDx (0-3, 4-5, 6), HTI (0-6)</p> <p>MSTID: MSTIDx (0-23), CDSS (0-1)</p>
12/10/2017	5.4%	 <p>EGNOS-D: 0-1 (Red), 2-23 (Green)</p> <p>Indicators: AATR (0-1, 23), TEC grad (0-1, 23)</p> <p>LSTID: HF-TID (0-1, 2-3, 4-5, 10-14), HF-INT (0-1, 2-16, 17-18, 19-20, 21-22, 23), LSTIDx (0-1, 23), HTI (0-1, 23)</p> <p>MSTID: MSTIDx (0-23), CDSS (0-1)</p>

Date	EGNOS-D	Time Interval
13/10/2017	13.10%	
07/11/2017	4.3%	
08/11/2017	11.2%	
24/11/2017	14.4%	

Date	EGNOS-D	Time Interval
12/12/2017	7.7%	 <p>EGNOS-D: 0-16h Green, 16-23h Orange, 23h Green</p> <p>Indicators: AATR (16-18h Green, 18-20h Red, 20-21h Yellow), TEC grad (16-21h Red)</p> <p>LSTID: HF-TID (0-23h Green), HF-INT (0-1h Yellow, 1-5h Green, 5-6h Red, 6-7h Yellow, 7-23h Green)</p> <p>MSTID: MSTIDx (0-9h Green, 9-14h Red, 14-23h Green), CDSS (16-21h Yellow)</p>
17/12/2017	16.6%	 <p>EGNOS-D: 0-17h Green, 17-23h Red</p> <p>Indicators: AATR (17-21h Red, 21-23h Yellow), TEC grad (17-23h Yellow)</p> <p>LSTID: HF-TID (16-17h Green, 17-18h Yellow, 18-19h Red, 19-20h Yellow, 20-21h Red, 21-23h Yellow), HF-INT (0-6h Green, 6-7h Yellow, 7-8h Green, 8-9h Yellow, 9-10h Green, 10-11h Yellow, 11-12h Green, 12-13h Yellow, 13-14h Green, 14-15h Yellow, 15-16h Green, 16-17h Yellow, 17-18h Red, 18-19h Yellow, 19-20h Red, 20-21h Yellow, 21-23h Red)</p> <p>MSTID: MSTIDx (0-23h Green), CDSS (0-23h Green)</p>
26/12/2017	6.0%	 <p>EGNOS-D: 0-13h Green, 13-15h Orange, 15-23h Green</p> <p>Indicators: AATR (13-15h Green), TEC grad (13-15h Green)</p> <p>LSTID: HF-TID (0-23h Green), HF-INT (0-23h Green)</p> <p>MSTID: MSTIDx (0-9h Green, 9-14h Red, 14-15h Orange, 15-23h Green), CDSS (13-15h Red)</p>

Results in Table 12 can easily observe the different scenarios for coincident degradation in EGNOS-D with disturbances detected by the TechTIDE methods/products as well as the different scenarios reporting ionospheric activity that do not impact on EGNOS-D. Table 12 results' confirm the very good agreement when compare the Disturbance Indicators with EGNOS-D, as expected as per [RD-5], [RD-7]. MSTID products reports also simultaneous activity when EGNOS-D is disturbed. The agreement of the activity detected by MSTID with EGNOS-D is much less good as for the Disturbance Indicators. This might indicate that MSTID can affect the performance of EGNOS but in a lesser impact as the one caused by ionospheric disturbances monitored by the AATR and GNSS-TEC Gradients. Some of the observed disagreements between EGNOS-D and MSTID-Detection might be caused by the fact that additional causes could increase the underperformance of EGNOS and because the MSTID detection have been referred to central Europe. LSTID products report some TID activity when EGNOS-D is disturbed but agreement is not as good as reported for the the Disturbance Indicators. We often observe LSTID activity events that do not report any disturbance on EGNOS-D, indicating that LSTID activity have no always impact on the EGNOS performance.

Results in Table 12 shows that for most of the scenarios when EGNOS suffer a degradation, the LSTID-Detection observes TID activity. However, many of the TID events detected by LSTID and MSTIDs causes no impact on EGNOS-D. This would indicate that LSTIDs events, and even MSTIDs, doesn't affect much EGNOS availability (EGNOS should rely on other Ionospheric disturbances).

To summarize the above results Table 13 shows the percentage of events detected by the TechTIDE method/products that report degradation in the EGNOS performance for the scenarios presented in Table 12, as well as the percent of disturbance events detected by the respective TechTIDE methods that do not impact in the EGNOS performance, the so called Undisturbed EGNOS-D.

Table 13. Percentage of Disturbed events detected by the respective TechTIDE method/products that coincide with degradation in the EGNOS performance (percentages in parenthesis refer to the ration of events when the particular method provide data) and with no with degradation in the EGNOS performance. Results in this table do not distinguish the degree of impact in the EGNOS performance. N/A means that no data is available for the given method/product.

	Method/Product	Disturbed EGNOS-D	Undisturbed EGNOS-D
Disturbance Indicators	AATR	86%	N/A
	TEC-Gradient	76%	N/A
LSTID Methods	HF-TID	61% (75%)	14%
	HF-INT _{EUx}	66%	21%
	LSTID-Index	68% (70%)	N/A
	HTI	45% (47%)	N/A
MSTID Methods	MSTID _x	29% (31%)	46%
	CDSS-MSTID	37% (100%)	N/A

The best agreement with EGNOS degradation are the disturbance indicators with percentage over 75%, the LSTID methods have and agreement over 60% (with the exception of HTI method) and MSTID methods have less percentage of agreement, around 30%. Note that MSTID methods refer to central Europe only and that CDSS-MSTID in particular report many scenarios with unavailable data, more than half of the scenarios analyzed. Concerning the disturbance detected by the TechTIDE methods that do not coincide with degraded performance in EGNOS, only HF-TID, HF-INT and MSTID_x report data. This indicate that not all LSTIDs events, and even MSTIDs, affect EGNOS availability. MSTID index reported a major number of TID scenarios without EGNOS affectation, maybe because in this tables MSTID index focused in central Europe. The latter results would indicate that most of the mechanisms related to ionospheric disturbances that causes EGNOS degradation are responsible also for

generation of LSTIDs and MSTIDs; e.g. intense geomagnetic storms as the one occurred for 7-8 September 2017 [RD-4].

The above analysis have been extended by comparing the strongest events detected by the HF-INT method ever since January 2018. Table 14 compare the events detected by HF-INT in real-time with detected events with other TechTIDE method/products and with potential impact on the EGNOS performance.

Table 14. List of scenarios when HF-INT method detects the strongest LSTID events since 2018. Comparison with other TechTIDE detection methods and with the impact on EGNOS, based on APV-I 99% Availability Degraded Area (EGNOS-D) is provided. N/A means that no data was available for the given method/product.

Date	HF-INT _{EUx}	HTI	MSTIDx	CDDS-MSTID	EGNOS-D
08/01/2018	TID	Uncertain	Weak	N/A	No Impact
15/02/2018	TID	No TID	Strong	N/A	No Impact
19/02/2018	TID	No TID	Strong	N/A	Impact
27/02/2018	TID	N/A	Strong	N/A	Impact
18/03/2018	TID	TID	Strong	TID	Impact
23/03/2018	TID	TID	Weak	TID	Impact
05/04/2018	TID	No TID	Weak	N/A	No Impact
10/04/2018	TID	TID	Weak	TID	Impact
22/04/2018	TID	No TID	Weak	N/A	No Impact
02/09/2018	TID	TID	No TID	N/A	Impact
03/09/2018	TID	No TID	No TID	N/A	No Impact
04/09/2018	TID	No TID	Strong	TID	Impact
10/09/2018	TID	Uncertain	Weak	N/A	No Impact
11/09/2018	TID	Uncertain	Weak	N/A	No Impact
13/09/2018	TID	TID	Strong	N/A	No Impact
01/10/2018	TID	No TID	Weak	N/A	No Impact
07/12/2018	TID	No TID	Weak	N/A	No Impact
08/12/2018	TID	Uncertain	Weak	N/A	No Impact
15/01/2019	TID	No TID	Weak	N/A	No Impact
16/03/2019	TID	TID	No TID	N/A	No Impact
26/03/2019	TID	No TID	No TID	N/A	No Impact

Date	HF-INT _{EUx}	HTI	MSTID _x	CDSS-MSTID	EGNOS-D
04/04/2019	TID	No TID	No TID	N/A	No Impact
15/04/2019	TID	No TID	Weak	N/A	No Impact
24/04/2019	TID	No TID	Weak	N/A	No Impact
28/04/2019	TID	No TID	No TID	N/A	No Impact
01/09/2019	TID	Uncertain	Strong	N/A	Impact
24/09/2019	TID	TID	Strong	N/A	No Impact
27/09/2019	TID	TID	Strong	N/A	Impact
01/10/2019	TID	No TID	Weak	TID	N/A
11/10/2019	TID	No TID	Weak	TID	N/A

As above, HTI method provides information above 5 single stations in Europe (Section 3.6). In this sense, in Table 14, we have considered that HTI detects TID activity if 3 or more stations report some activity, uncertain if only 2 or less detects some activity and no TID for remaining cases. Concerning MSTID_x, we indicate in the Table 14 the MSITID_x for central Europe. Finally, as refers to the information of the CDSS-MSTID product, we have to consider that results are only relevant for the Czech Republic (western part) and that most of the time scenarios specified in Table 14 fit into periods when foF2 < 4.65 MHz; hence, no information is available using CDSS-MSTID at 4.65 MHz. The results of Table 14 confirm that all given scenarios reporting impact on EGNOS performance are characterized by TID activity, all TechTIDE Methods detect TIDs. However, not all scenarios with TID activity result with an impact on the EGNOS performance. Table 15 shows the percentage of events with coincided TID activity detection by the given TechTIDE methods and with degradation in the EGNOS performance for the scenarios presented in Table 14.

Table 15. Percent of scenarios reported in Table 14 with simultaneous TID detection by given methods. The last column reports the percent of scenarios that a given method detects TID activity and EGNOS performance is degraded.

	HF-INT _{EUx}	HTI	MSTID _x	CDSS-MSTID	EGNOS-D
HF-INT _{EUx}	100 %	50 %	80 %	100 %	32 %
HTI	50 %	100 %	60 %	50 %	67 %
MSTID _x	80 %	60 %	100 %	100 %	54 %
CDSS-MSTID	100 %	50 %	100 %	100 %	100 %

Results of Table 15 confirms those of Table 13. Most of given scenarios reporting impact on EGNOS performance are characterized by TID activity (LSTID and MSTID). We often observe LSTID and MSTID activity events that do not report any disturbance on EGNOS-D, indicating

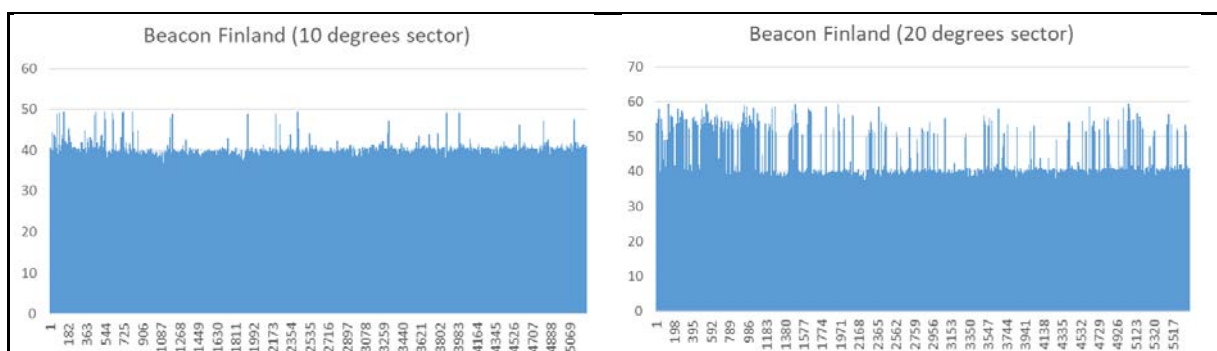
that LSTID activity have no always impact on the EGNOS performance. However, many of the TID events detected by LSTID-Methods causes no impact on EGNOS-D. Again, this is indication that LSTIDs and MSTIDs events doesn't affect much EGNOS availability, and that impact on EGNOS performance should rely more on other Ionospheric disturbances.

4.2. Impact of TechTIDE TID detection on ground systems

In order to analyze the impact of TID detected by TechTIDE method/products on ground systems we focus our analysis on direction finding measurements performed by the GFP. We refer the reader to Section 2.2.2 of [RD-5]. GFP provided measurements of azimuths recorded by his HF Direction Finder (DF) for given HF beacons.

As already known DF measurements have the challenge that the DF sometimes receives HF signals transmitted by different emitter and thus indicating azimuths from a completely different directions. GFP provided with DF measurements that took place during a timeframe reported as influenced by a TID event, as detected by HF-INT method of TechTIDE. However, the beacon measurement started in June 2019 for the HF beacons in Madeira and Finland and in December 2017 for the HB beacon in Kaliningrad. The real azimuth value of the beacons from the DF of the GFP to the analyzed HF transmitters are 58.882° , 233.194° , and 39.467° for Kaliningrad, Madeira, and Finland respectively. We have to consider that DF measurements are not performed systematically and few scenarios for which coincide a TID event with DF measurements could be analyzed.

The DF measurements of the GFP were filtered in differently narrow sectors (+/- 10 degrees, 20 degrees, 30 degrees and 360 degrees to focus on the HF transmitting beacon of interest. Data shown in Figure 18 correspond to the azimuth measurements by applying different sector filters centered on the azimuth direction of the HF beacon in Kaliningrad. Note that a sector defined of 360° means no filtering at all and the HF direction finder provides histograms of signals received in any direction. Figure 18 clearly shows that narrowing the filter, DF measurements of azimuths are more and more related to the HF beacon of interest.



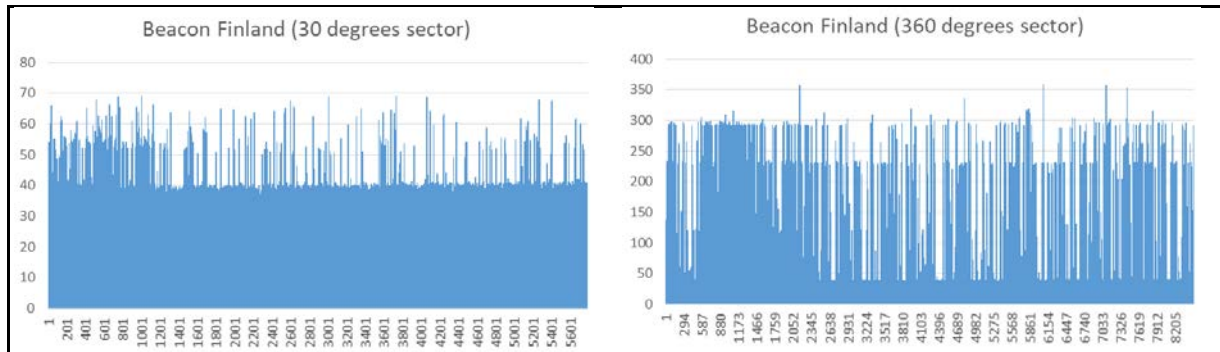


Figure 18. Histograms reporting the number of measurements (x-axis) observed with a given azimuth (y-axis). The different filters have been applied in the direction azimuth of the indicated HF Beacon and with the given aperture of sector as noted in the legend.

The DF measurement values were grouped into bins that correspond to a given TID timeframe, the so called “TID-bin”, and the average squared deviation ($AvSQD_{TID}$) have been calculated for such scenarios in order to have a metric which tells us about the quality of the DF measurements. All the other measurements were put in another bin, the so called “No-TID-bin” for which the average squared deviation was calculated as well ($AvSQD_{NoTID}$). Therefore, we have the quality of DF measurement for given TID-bin and for no TID-bin. The smaller the $AvSQD$ the better quality of DF measurement. Having this information we consider that a DF measurement is **degraded** by a TID event if $AvSQD_{TID} > AvSQD_{NoTID}$ and **no degraded** otherwise.

Analysis of LSTID events detected by the HF-INT method in TechTIDE are compared with DF data provided by GFPD. Unfortunately, there is few data available with coincident LSTID detections and DF data and found only 9 events whose results are provide in the Table 16.

Table 16. Analysis of the coincident TID events detected by HF-INT with DF measurements.

TID-Event	$AvSQD_{NoTID}$	$AZIM_{HF-B}$	$AvSQD_{TID}$	$AZIM_{TID}$	$\Delta AZIM$	Degraded
17/12/2017	17,6	58.9°	28,6	160 °	101.1 °	YES
08/01/2018	17,6	58.9°	6,7	190 °	131.1 °	NO
18/03/2018	17,6	58.9°	10.4	190 °	131.1 °	NO
23/03/2018	17,6	58.9°	58.6	150 °	91.1 °	YES
10/04/2018	17,6	58.9°	34.4	180 °	121.1 °	YES
01/09/2019	11.9	233.2°	16.1	170 °	63.2°	YES
24/09/2019	11.9	233.2°	14.4	200 °	33.2°	YES
11/10/2019	11.9	233.2°	4.4	220 °	13.2°	NO
11/10/2019	18.6	39.5°	0.9	220 °	180.2°	NO

Results presented in the Table 16 are limited but we can get to the conclusion that if a detected **TID** propagates close to **parallel** to the azimuth direction of the HF transmitter

beacons from the DF of the GFP then the **DF** measurements are **not degraded**. However, if the detected TID does not propagate close to the parallel to the azimuth direction of the HF transmitter beacons from the DF of the GFP then the quality of the DF measurements is degraded. Therefore, the more **perpendicular** TID propagation to the HF-link for DF measurements the higher **degradation**. Although we have only 9 coincident events of TID detection with the GFP-DF measurements, none of the analyzed events disagree with the above argumentation. It should be noted that events on 08/01/2018, 18/03/2018 and 24/09/2019 report LSTID propagating with angles that are neither close to parallel nor close to perpendicular to the azimuth direction of the HF transmitter beacons from the DF of the GFP. It should be noted that despite all the events are considered to have strong activity, the first two, occurred on 08/01/2018 and 18/03/2018, have half amplitude than the latest, occurred in 24/09/2019.

5. Summary and additional remarks

The deliverable presents a report on the final products in TechTIDE. The TID identification codes in TechTIDE have been adjusted since its first release driven by the assessment of the TID impact on aerospace and ground systems (WP5) to efficient support specific systems operations (such EGNOS, N-RTK, HF communication and geolocation) and the mitigation of the TID effects. The new products and improvements resulted of users' recommendations and WP5 results.

Large number of analysis have been performed concerning the occurrence of TIDs as detected by the TechTIDE methods and obtained a "climatology" that might serve to users to be warned about the largest occurrence of LSTIDs and MSTIDs Figure 19. MSTIDs have largest occurrence for midday with some significant occurrence after midnight. However, LSTIDs occurs dominantly by nighttime with some significant activity close to sunrise.

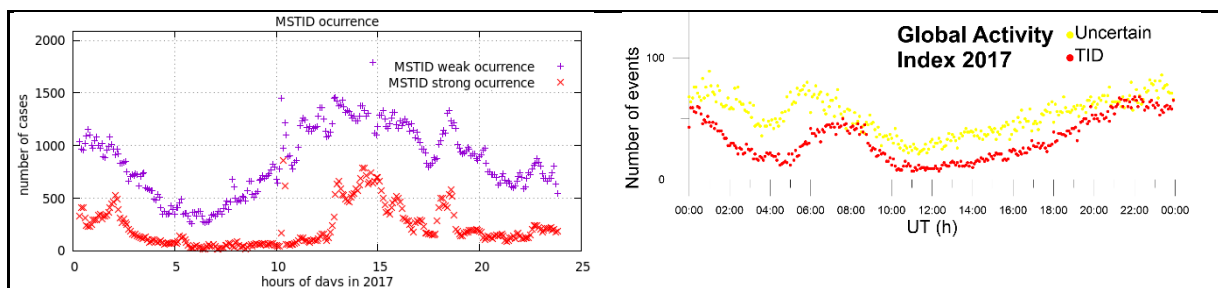


Figure 19. Distribution of the MSTID events detected by the MSTID_x (left) and of the LSTID events detected by HF-INT_{EUx} (right) for 2017.

The methods products will feed a warning system and establish a pre-operational system whose reliability of detection and to issue warnings of the occurrence of TIDs over the region extended from Europe to South Africa have been demonstrated. TechTIDE warning system will estimate the parameters that specify the TID characteristics and the inferred perturbation, with all additional geophysical information to the users to help them assess the risks and to develop mitigation techniques, tailored to their application. This document is a report for the



final products and improvements provided by TID identification codes in TechTIDE after its adjustment since its first release which resulted of users' recommendations and WP5 results.